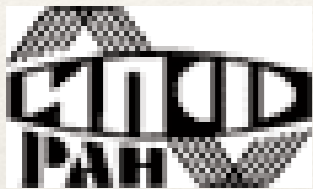




А. Соловьев¹, К. Бурдонов¹, А. Еремеев, В. Гинзбург, Е. Хазанов, А. Кочетков, А. Кузьмин, И. Шайкин, А. Шайкин, В. Яковлев, М. Стародубцев
М. Алхимова, Т. Пикуз, Е. Филиппов, С. Пикуз,
S. N. Chen^{1,2}, G. Revet², S. Pikuz³, E. Filippov³, M. Cerchez⁴, T. Gangly², and J. Fuchs^{1,2}

Исследования в области физики плазмы и ускорения частиц на субпетаваттном лазерном стенде PEARL

Collaborators



Соловьев А.А.¹
Бурдонов К.Ф.¹
Сладков А.Д.¹
Коржиманов А.В.¹
Гинзбург В.Н.¹
Хазанов Е.А.¹
Кочетков А.А.¹
Кузьмин А.А.¹,
Шайкин И.А.¹
Шайкин А.А.¹
Яковлев И.В.¹

Стародубцев М.В.



S. N. Chen^{1,2}
G. Revet²
J. Fuchs^{1,2}



Пикуз С.А.³
Скобелев И.Ю.³
Рязанцев С.Н.³
Алхимова М.А.³
Филиппов Е.Д.³
Пикуз Т.А.³



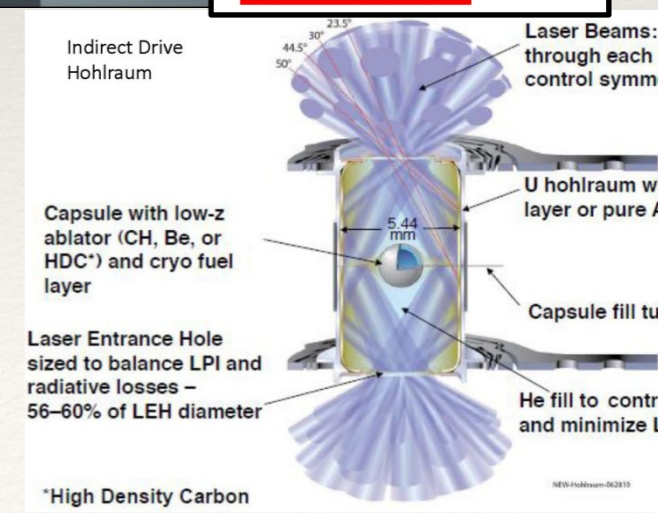
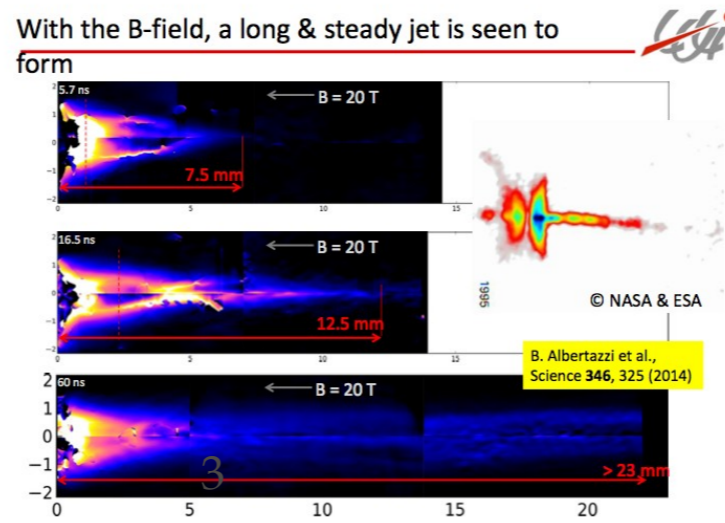
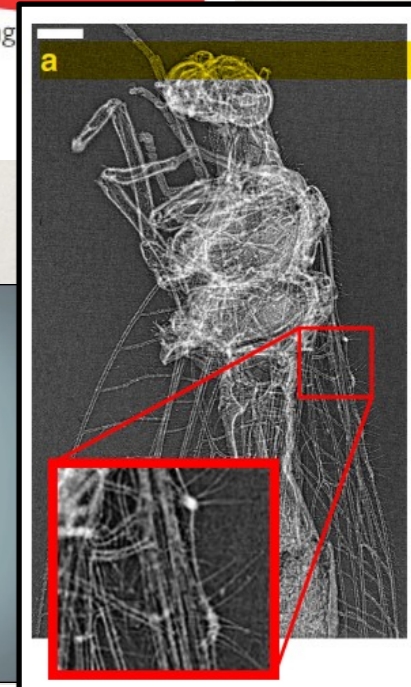
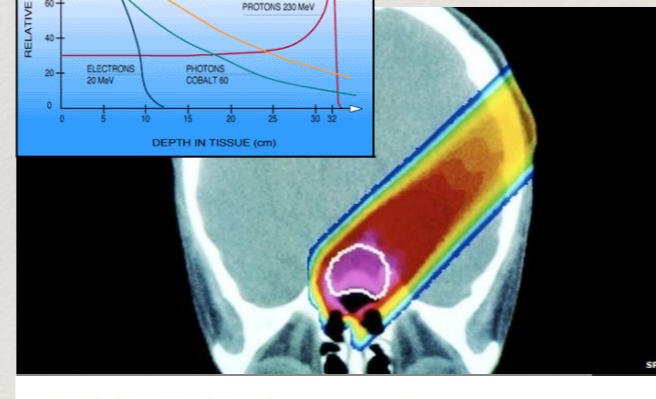
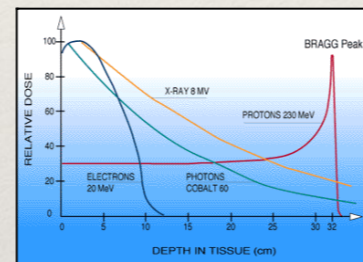
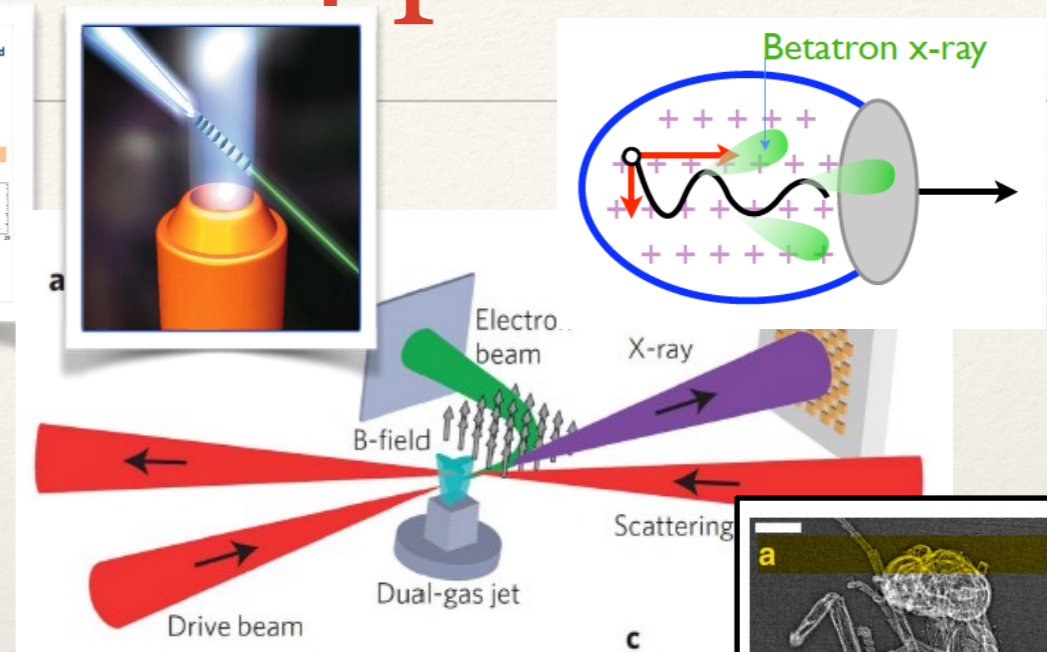
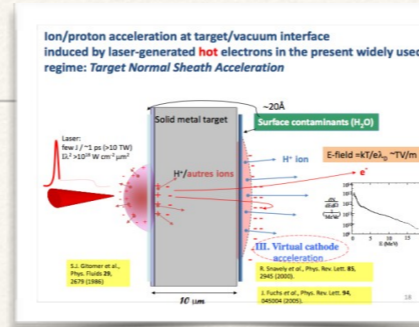
A. Chiardi⁴
B. Khair⁴



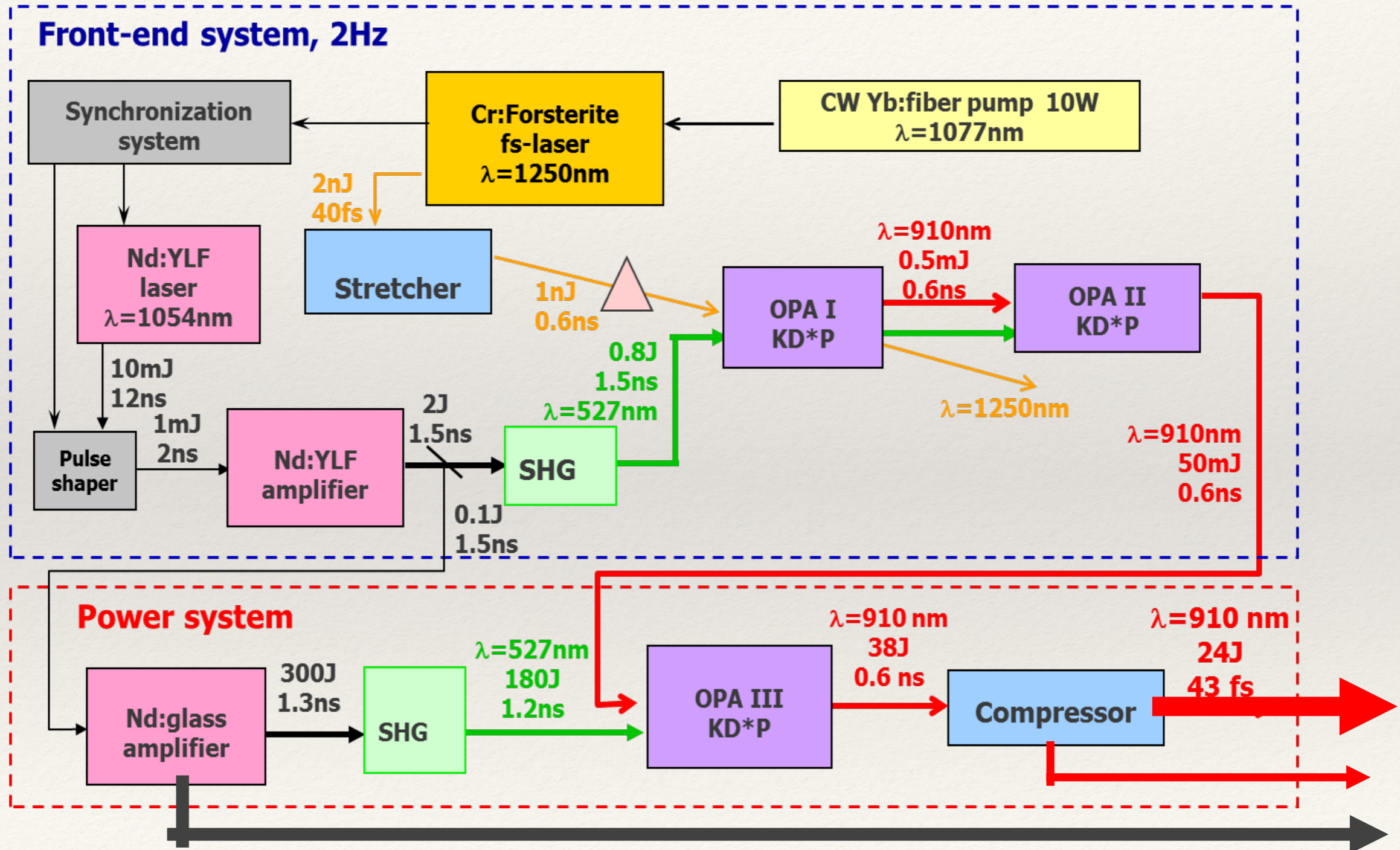
К.Л. Губский
А.П. Кузнецов

Laser-plasma interaction: applications

- ❖ Laser driven acceleration
- ❖ Particles acceleration
- ❖ X-ray generation.
- ❖ Applications
 - ❖ Radiotherapy
 - ❖ Bio-imaging
- ❖ HED physics
 - ❖ LabAstro
 - ❖ ICF



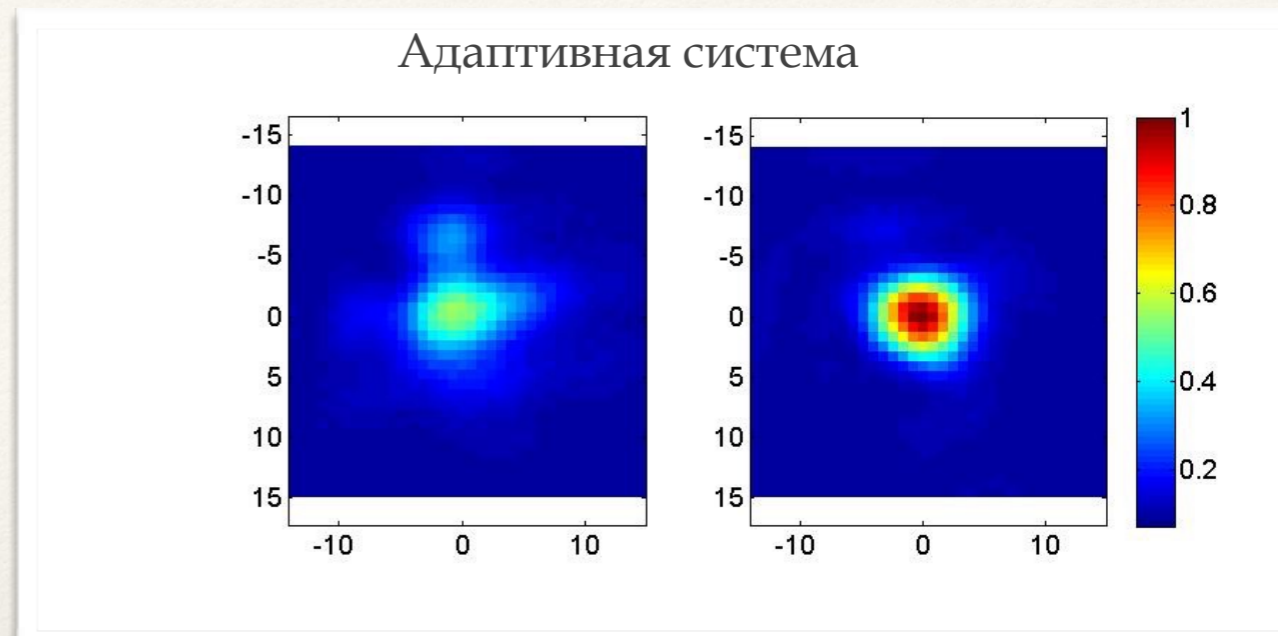
Sub-PW OPCPA PEARL laser facility



PEARL Ion acceleration

Ускорение протонов/ионов:

непрозрачная плазма (твердотельные мишени)
острая фокусировка лазерного излучения (высокая I)
высокий контраст лазерного излучения

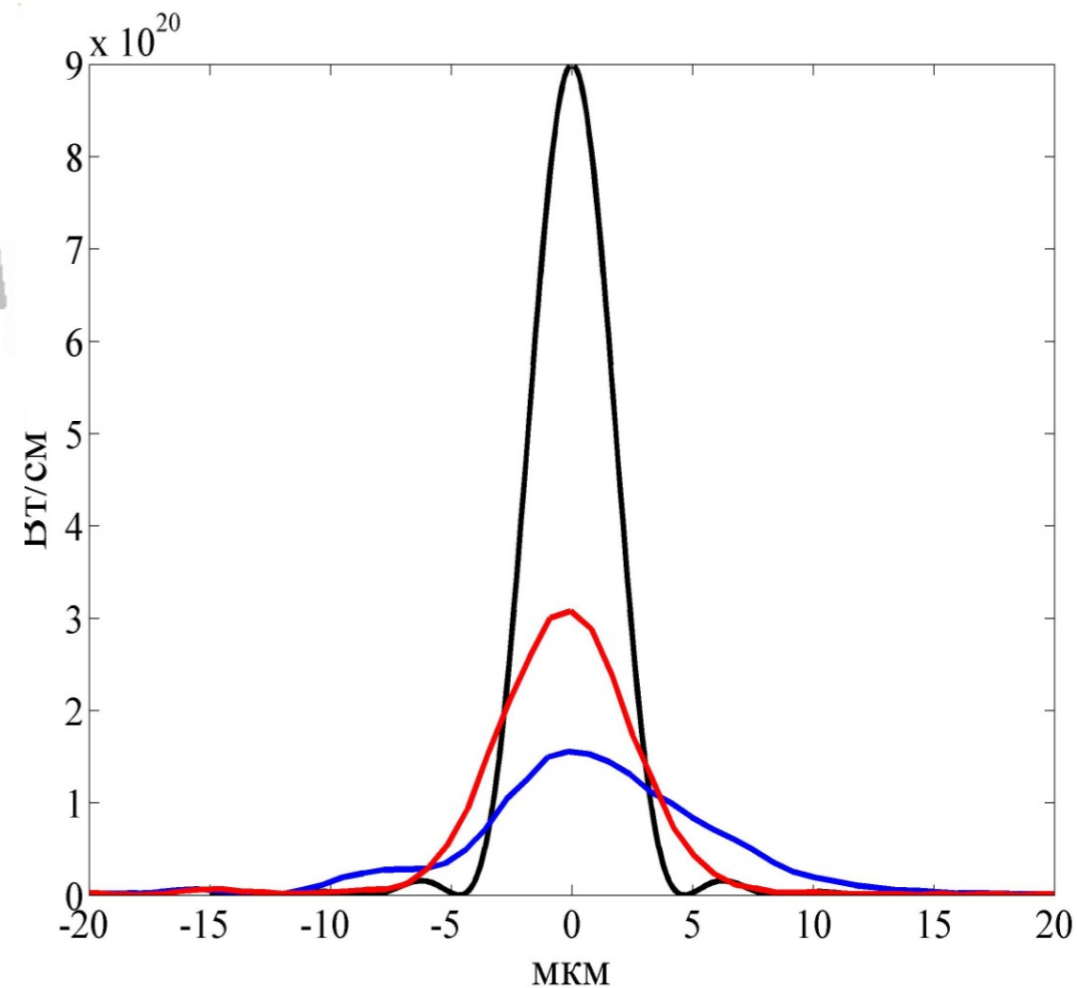
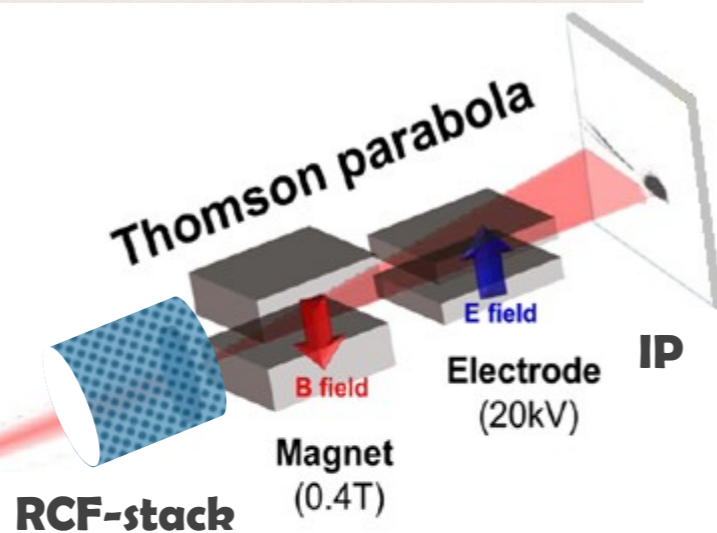


$\lambda_0 \approx 910 \text{ nm}$,
 $\tau \approx 60 \text{ fs}$,
 $E \approx 10 \text{ J}$,
 $P \approx 160 \text{ TW}$,
 $D \approx 100 \text{ mm}$,
Laser beam

$I \approx 3 \times 10^{20} \text{ W/cm}^2$
 $C > 2 \times 10^8 \text{ (1 ns)}$

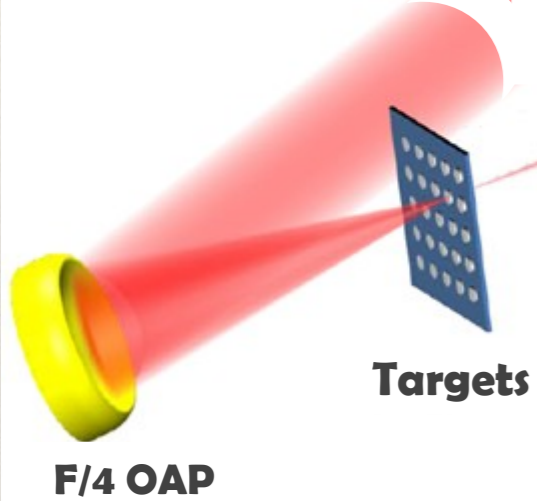
Targets

F/4 OAP

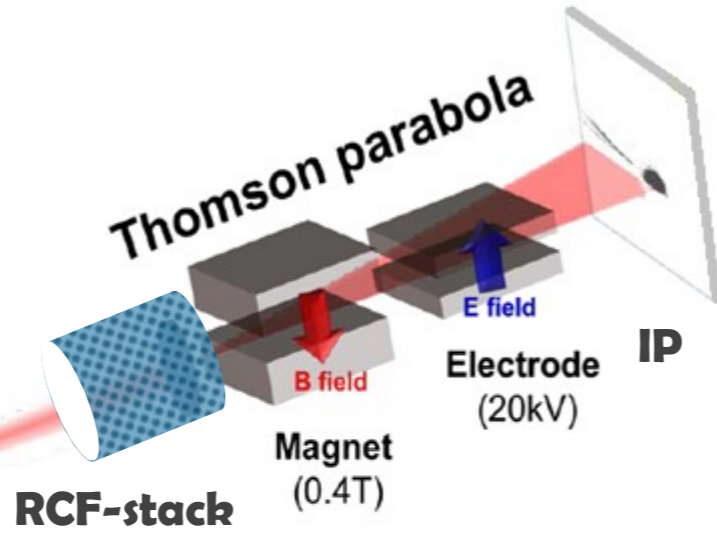
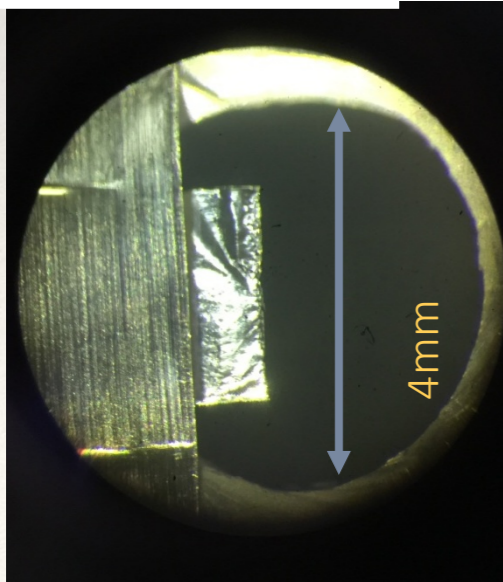


Ion acceleration

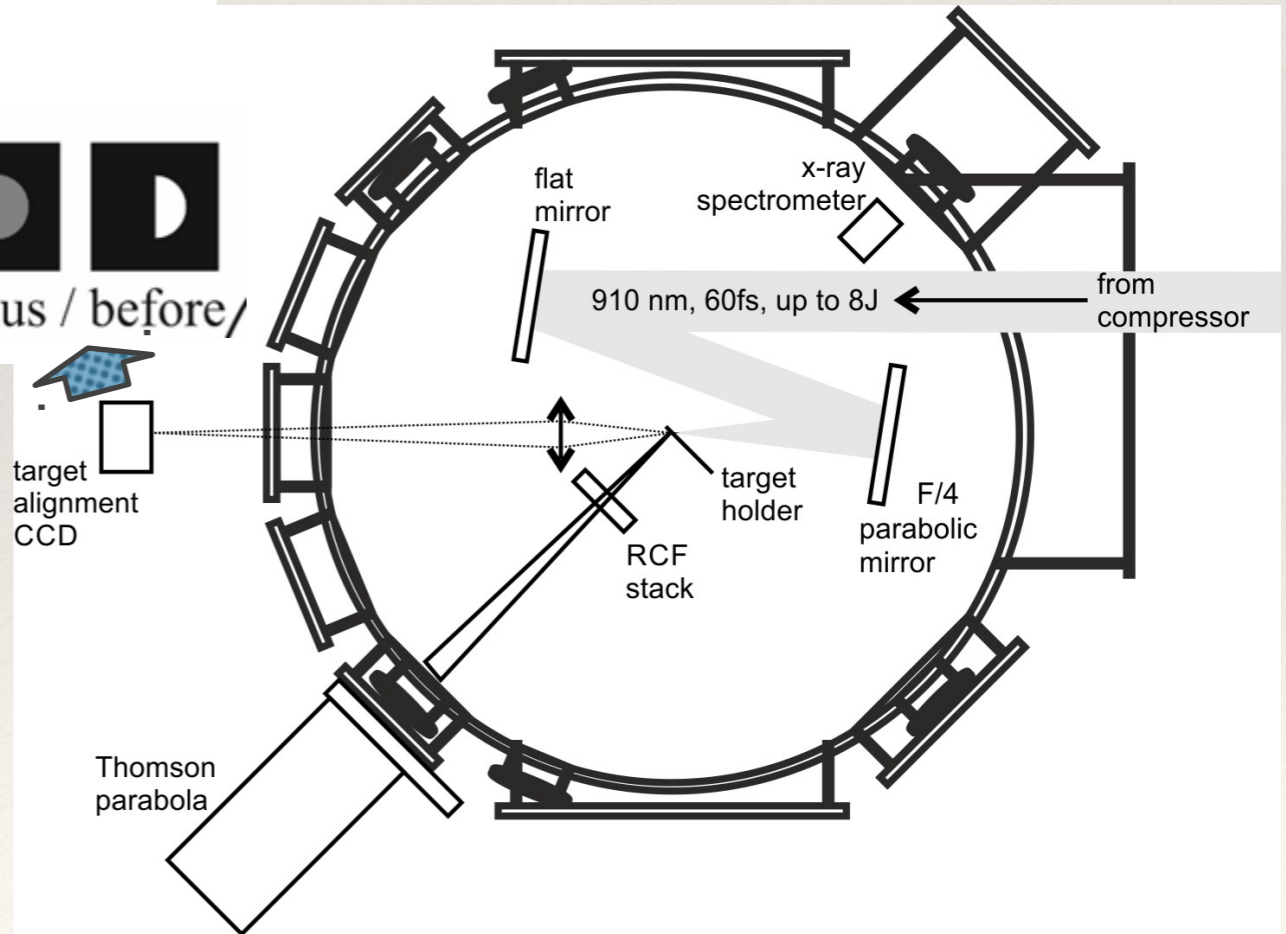
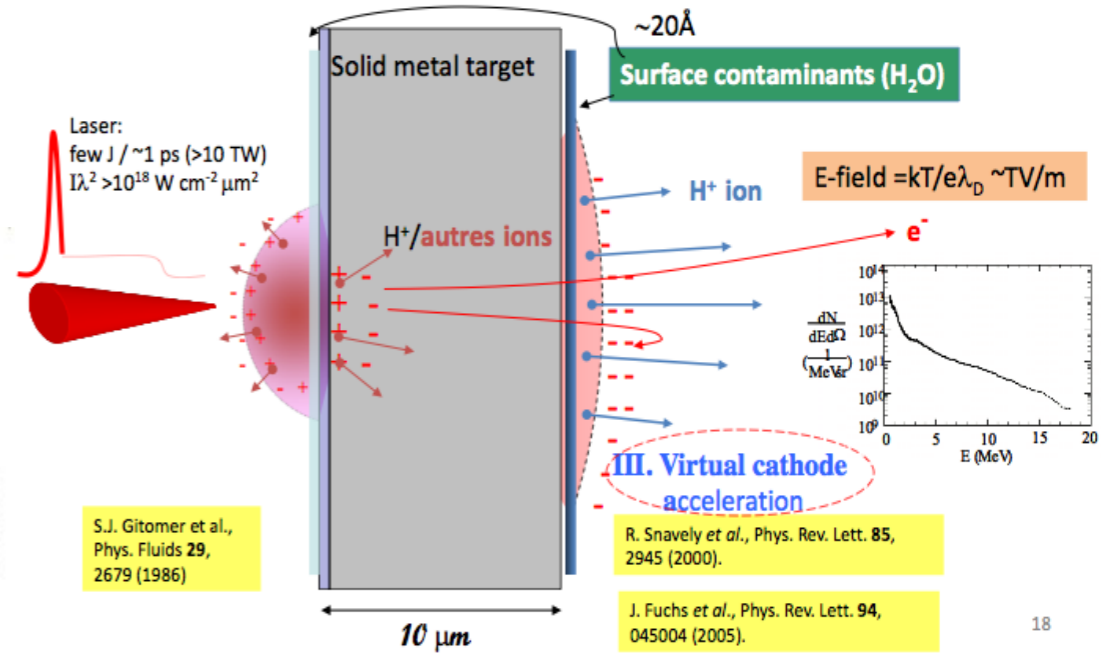
$\lambda_0 \approx 910 \text{ nm}$,
 $\tau \approx 60 \text{ fs}$,
 $E \approx 10 \text{ J}$,
 $P \approx 160 \text{ TW}$,
 $D \approx 100 \text{ mm}$,
Laser beam



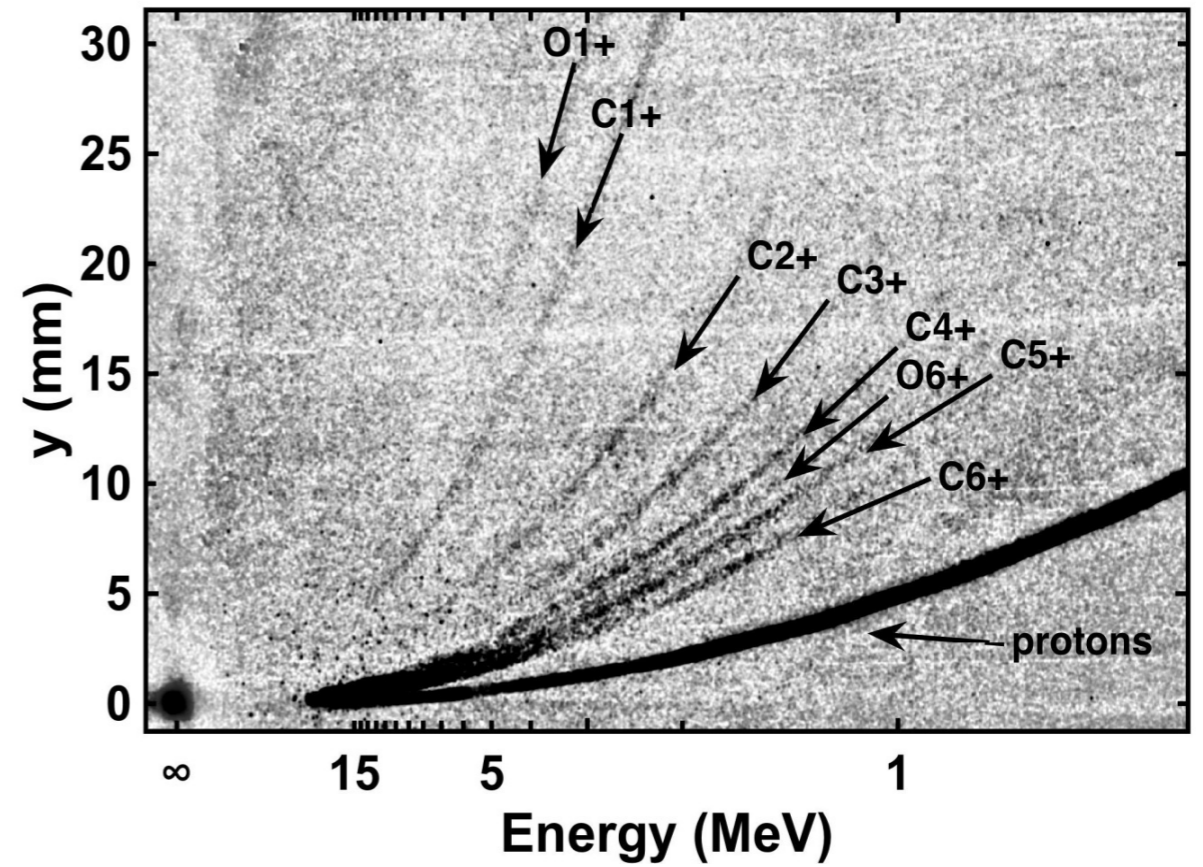
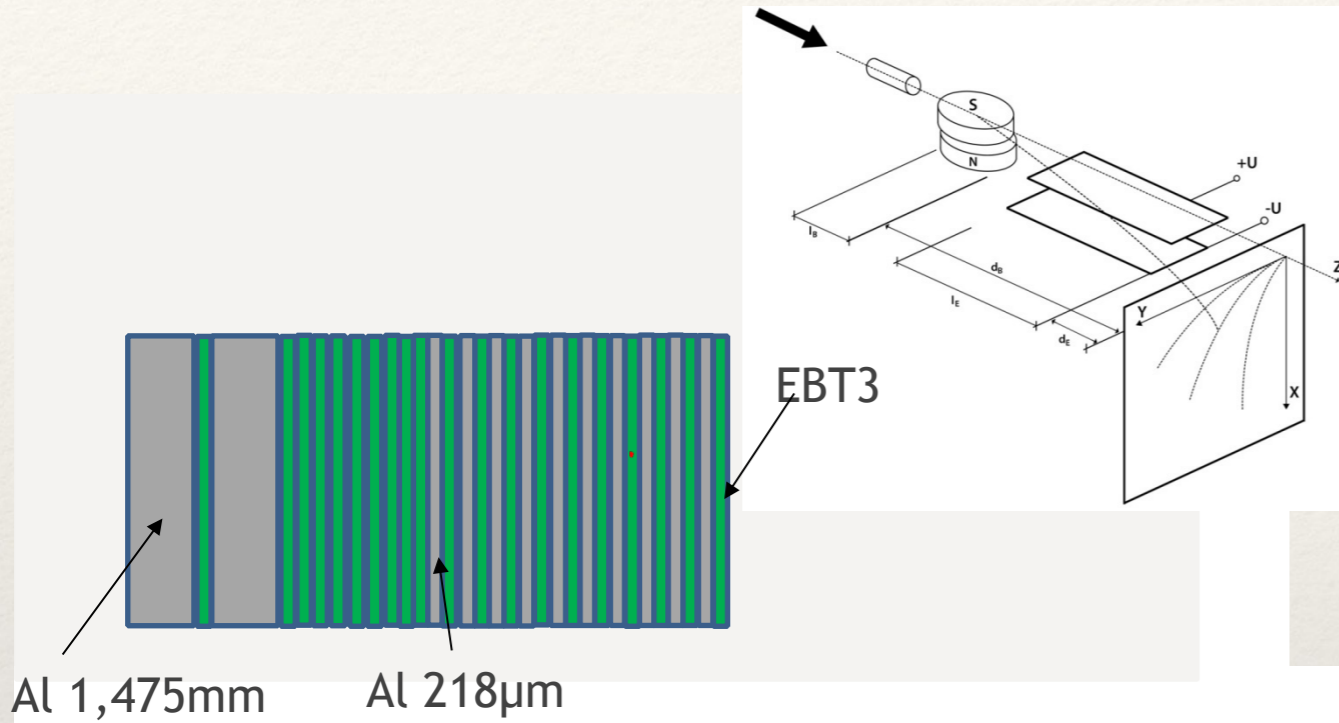
Sub-Rayleigh positioning



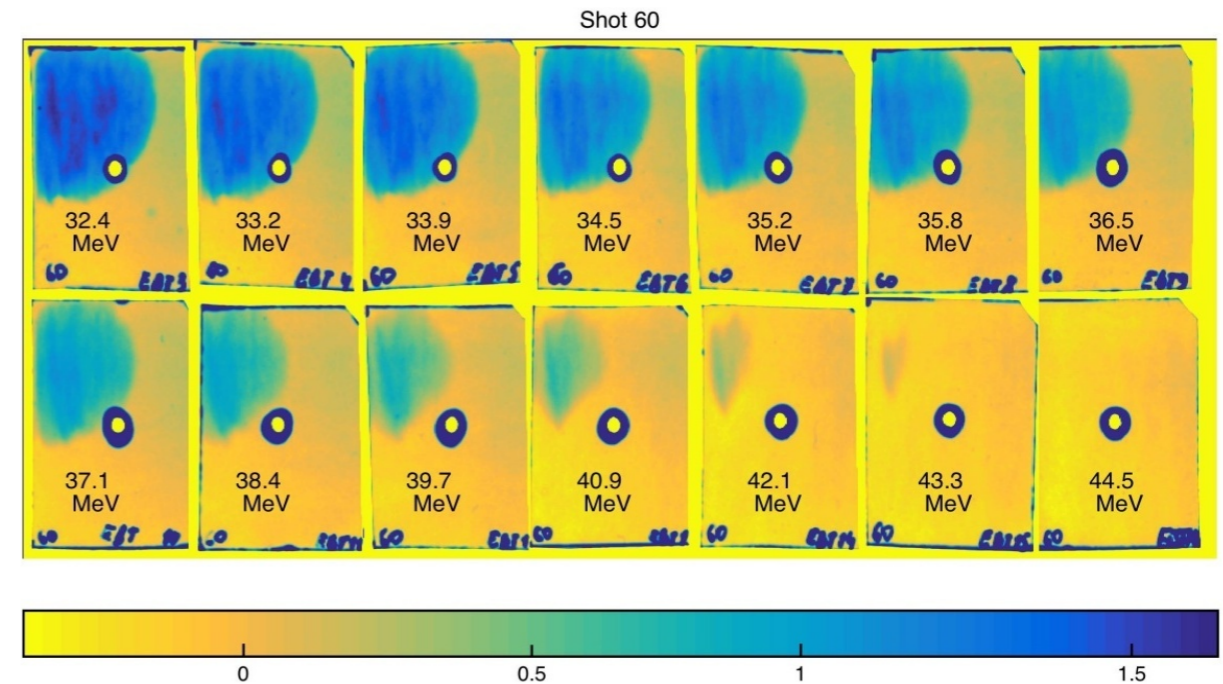
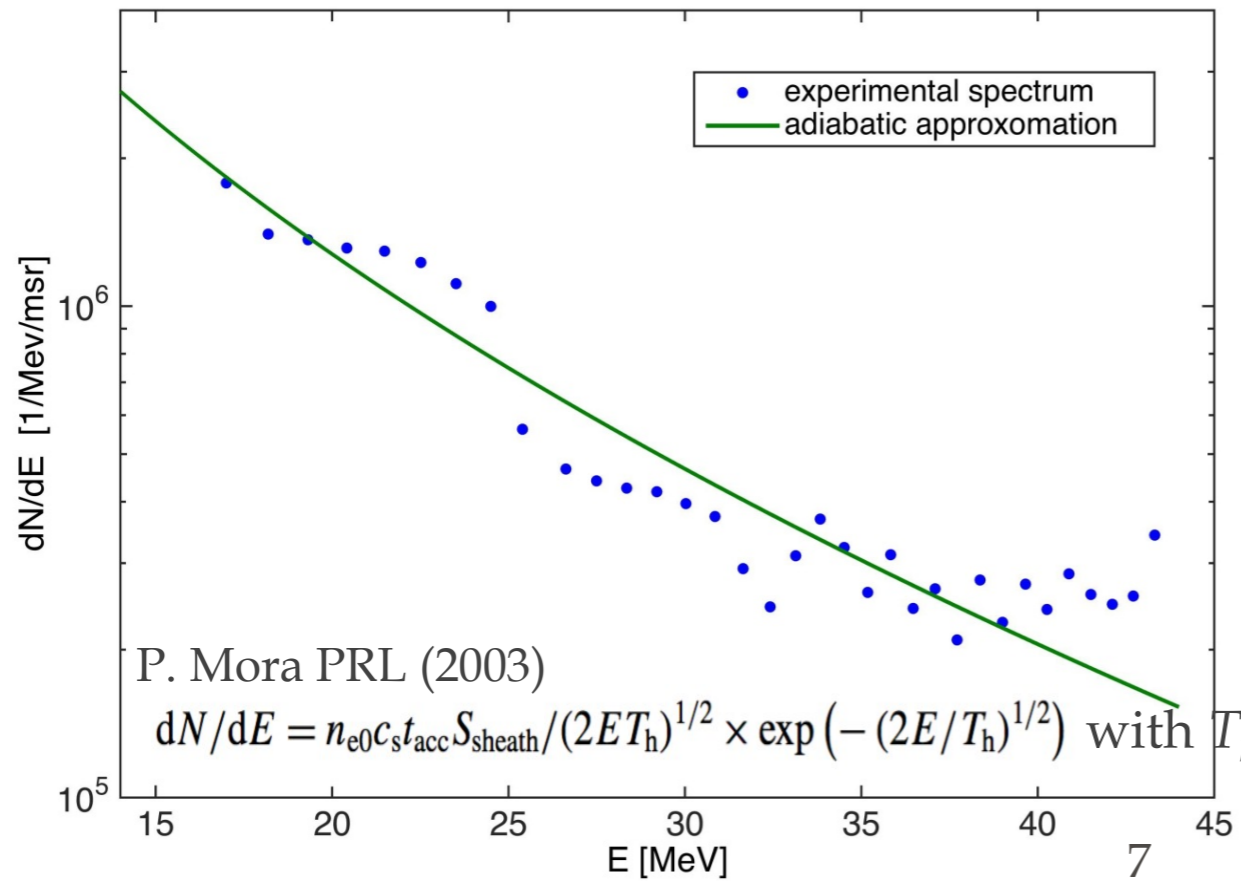
Ion/proton acceleration at target/vacuum interface induced by laser-generated **hot** electrons in the present widely used regime: **Target Normal Sheath Acceleration**



Ion acceleration

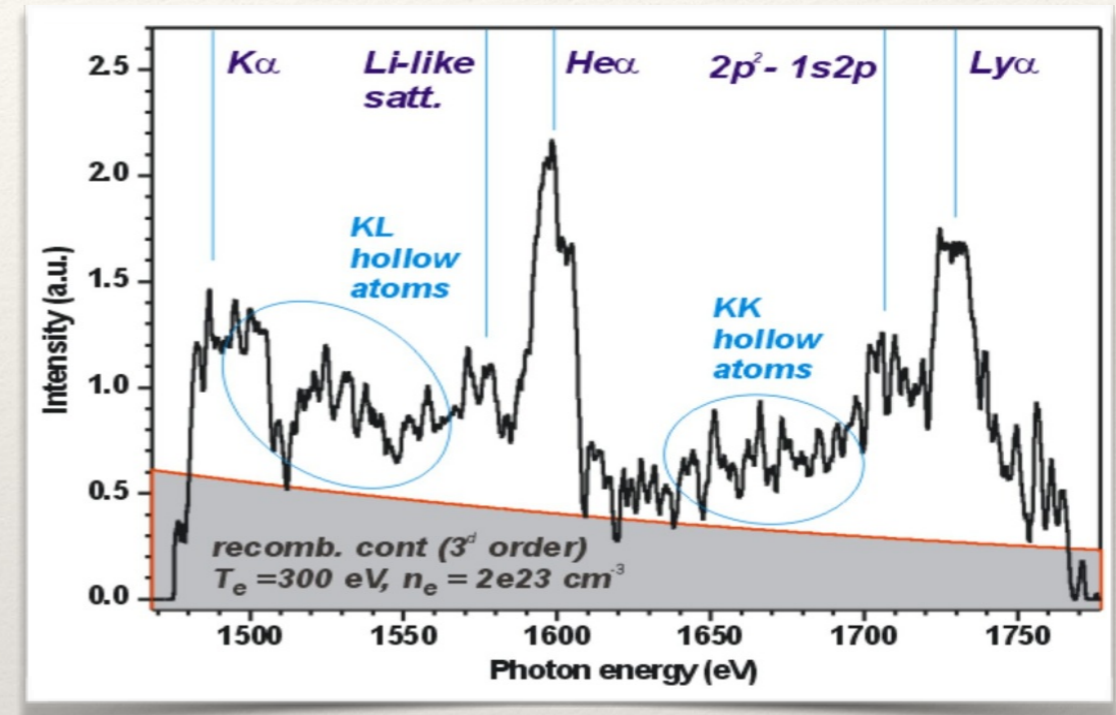
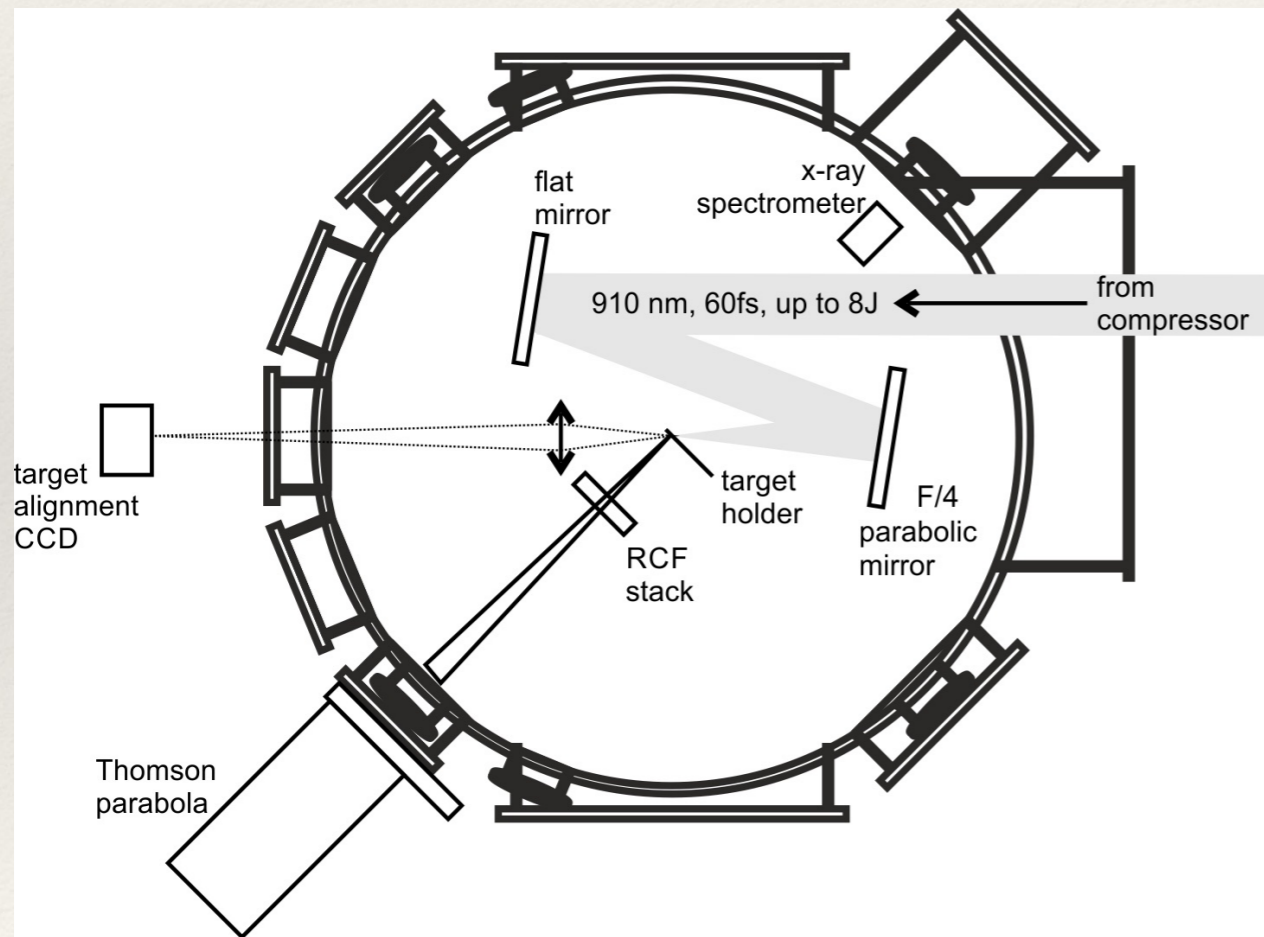


Experimental data:



Ion acceleration: X-ray spectrometry

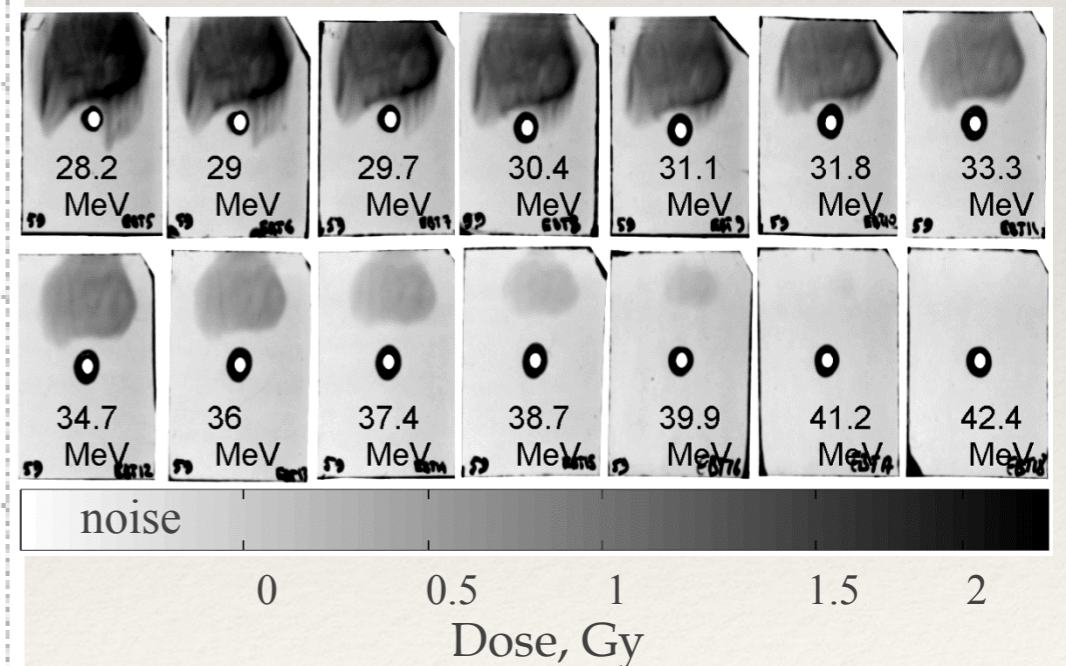
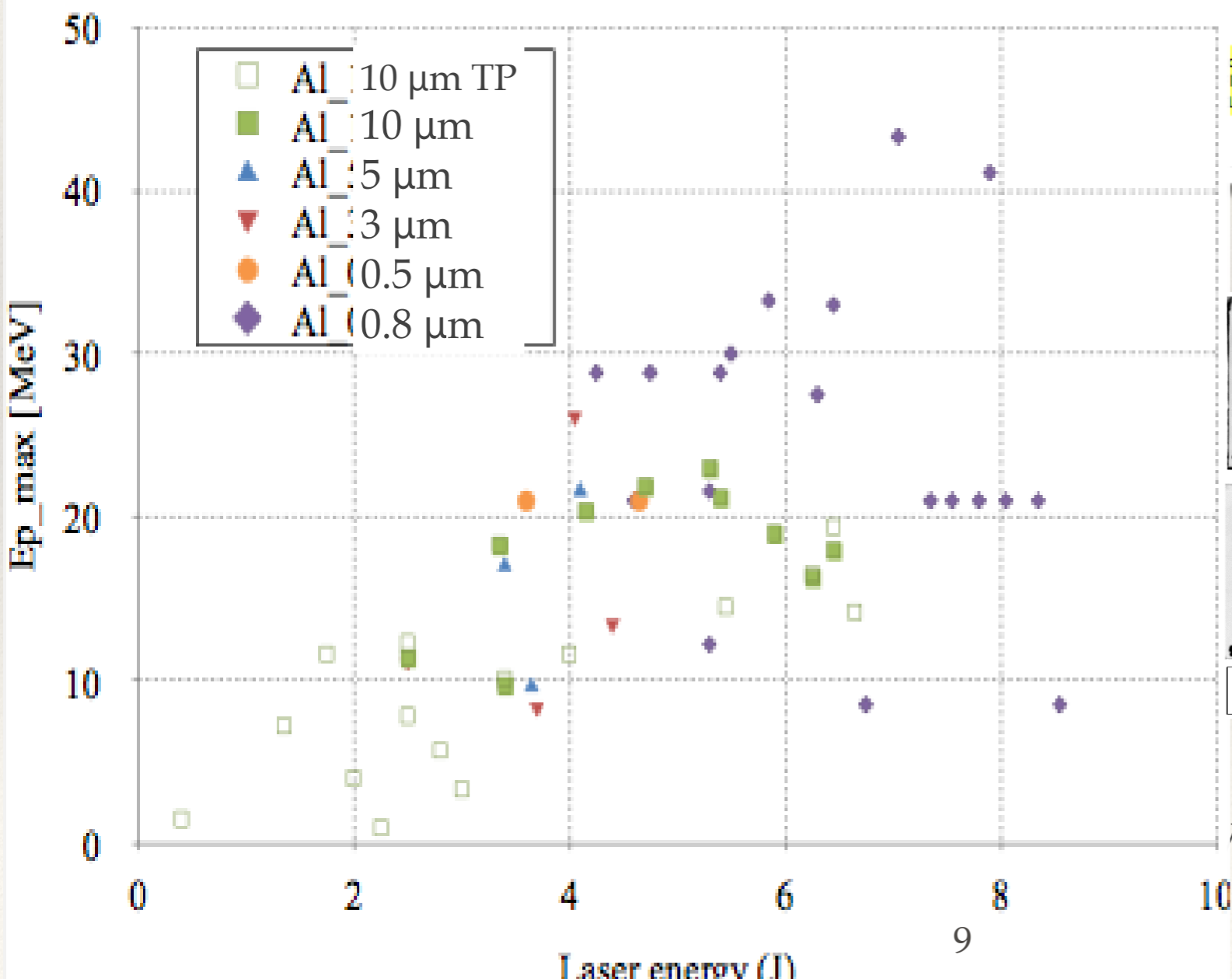
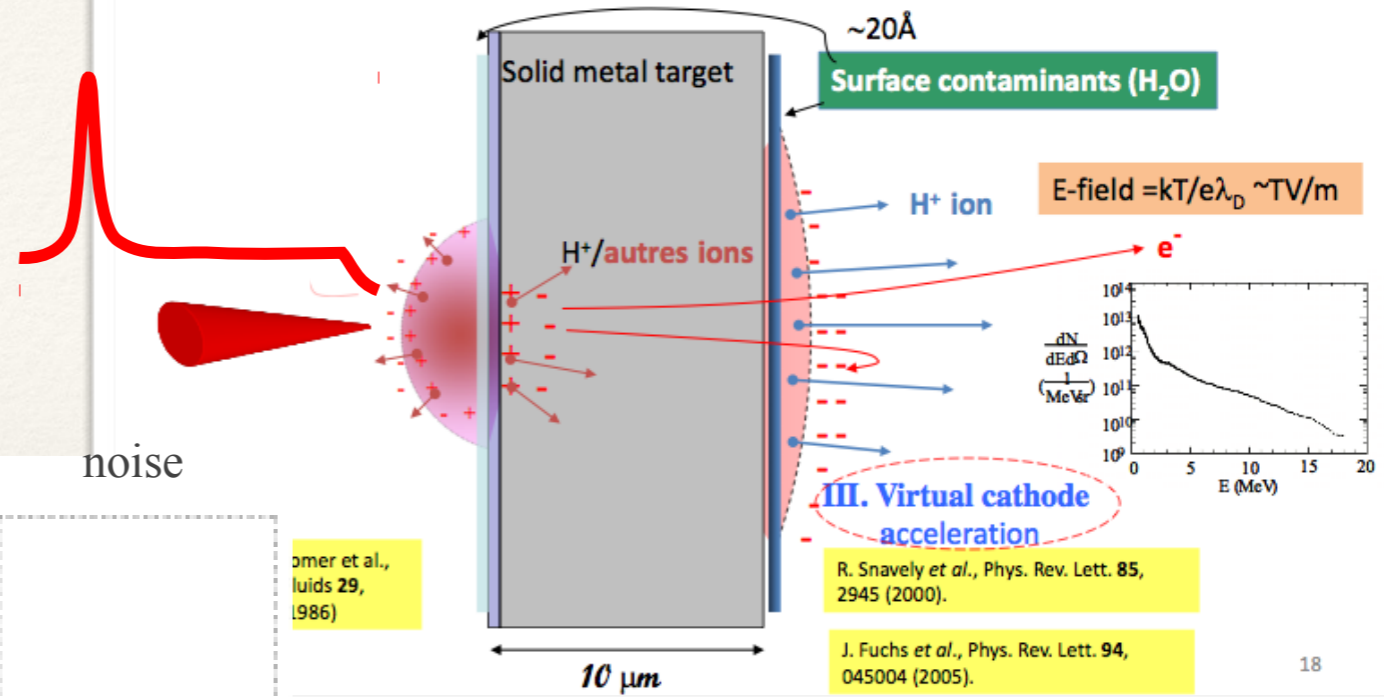
Focusing Spectrometer with Spatial Resolution (FSSR)



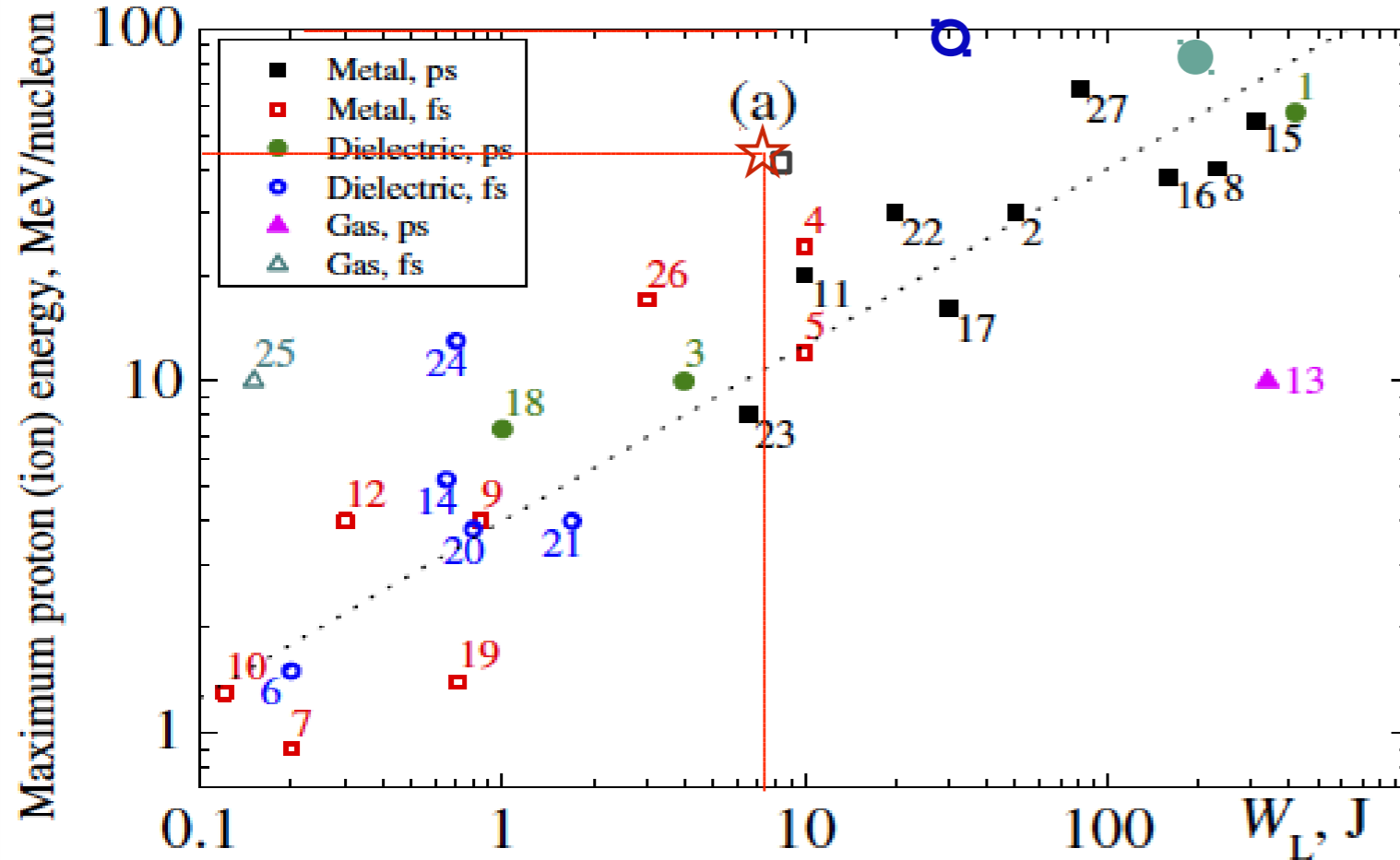
No signature of a significant preplasma at the target front:
the target remains at solid density by the time the main laser pulse arrives

Ion acceleration: statistics

Ion/proton acceleration at target/vacuum interface induced by laser-generated hot electrons in the present widely used regime: Target Normal Sheath Acceleration



43.3 MeV proton beam



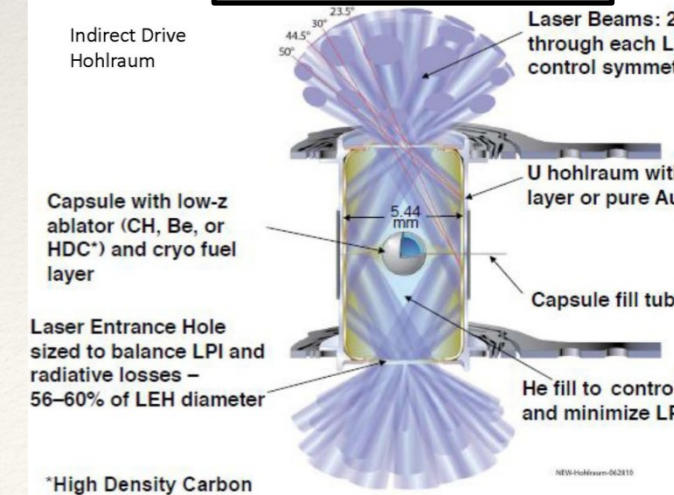
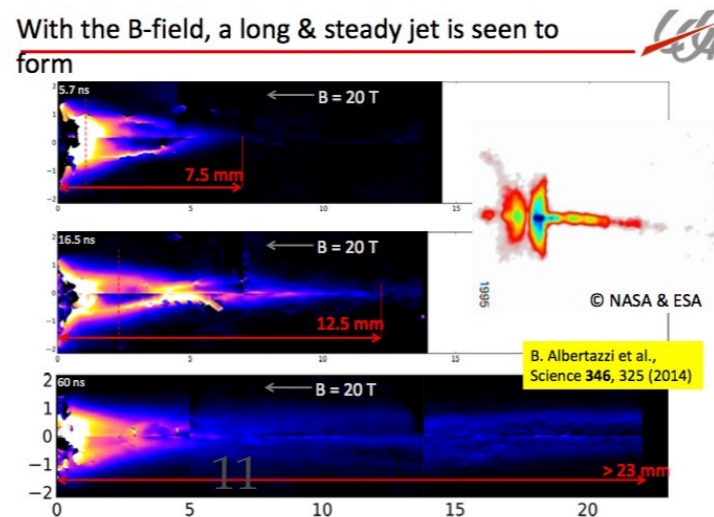
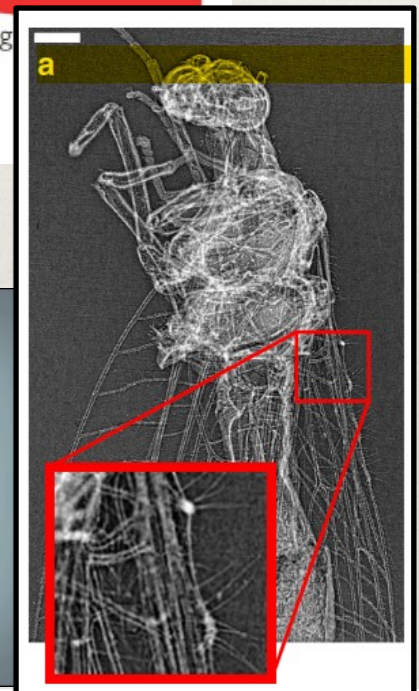
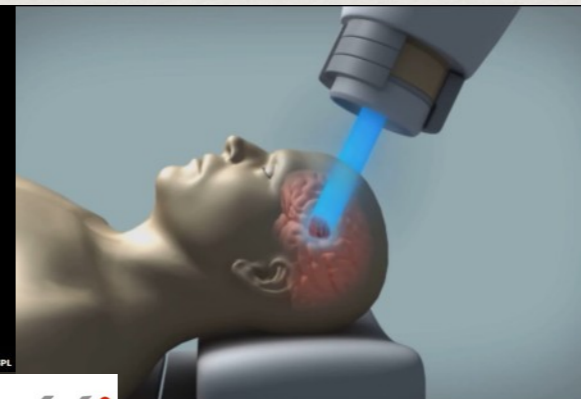
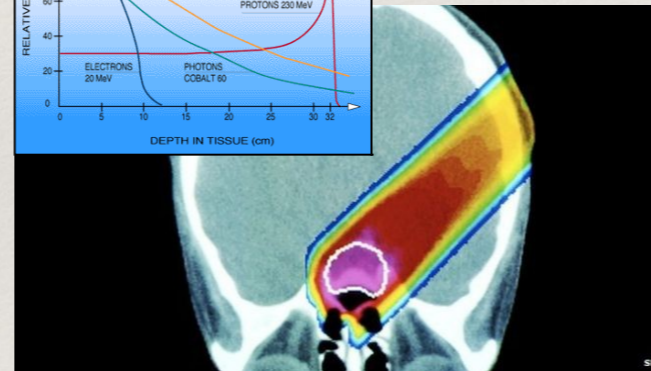
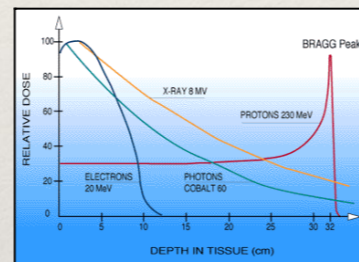
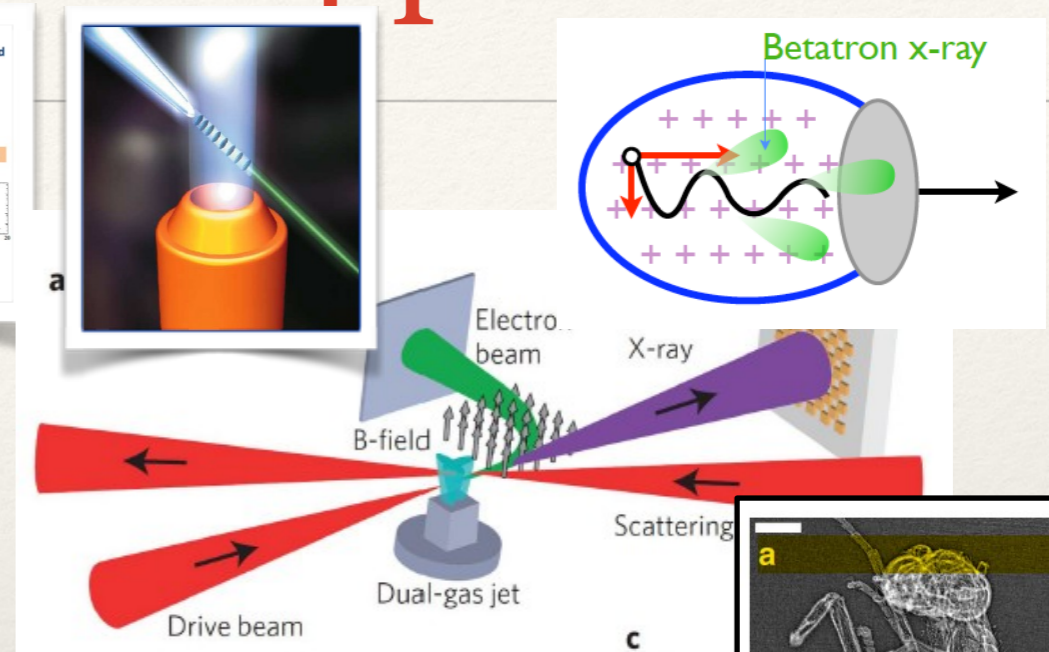
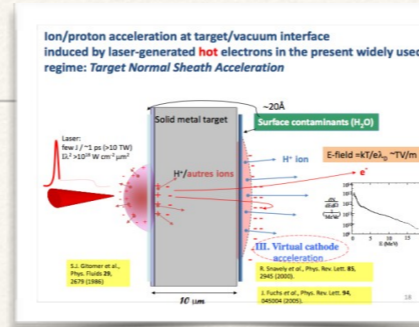
■ Ogura et al., Optics Letters 37 14 (2012)
 41 MeV - TNSA
★ IAP RAS summer 2015 (SR)
 43 MeV - TNSA
● Wagner et al, Phys Rev Letters 116 205002 (2016)
 85 MeV - TNSA
○ Jong Kim et al, Physics of Plasmas 23 070701 (2016)
 93 MeV – RPA (world record for today)

No.	Reference	Pulse energy W_L (J)	Pulse duration τ (fs)	Irradiance I_0 (W cm^{-2}) ^a	Contrast	Target and thickness (μm)	Incidence angle ($^\circ$)	Proton/ion energy $\mathcal{E}_{p(i)}$, (MeV/nucleon)
1	Snavely <i>et al</i> (2000)	423	500	3×10^{20}	1×10^4	CH 100	0	58
2	Krushelnick <i>et al</i> (2000b)	50	1000	5×10^{19}		Al 125	45	30
3	Nemoto <i>et al</i> (2001)	4	400	6×10^{18}	5×10^5	Mylar 6	45	10
4	Mackinnon <i>et al</i> (2002)	10	100	1×10^{20}	1×10^{10}	Al 3	22	24
5	Patel <i>et al</i> (2003)	10	100	5×10^{18}		Al 20	0	12
6	Spencer <i>et al</i> (2003)	0.2	60	7×10^{18}	1×10^6	Mylar 23	0	1.5
7	Spencer <i>et al</i> (2003)	0.2	60	7×10^{18}	1×10^6	Al 12	0	0.9
8	McKenna <i>et al</i> (2004)	233	700	2×10^{20}	1×10^7	Fe 100	45	40
9	Kaluza <i>et al</i> (2004)	0.85	150	1.3×10^{19}	2×10^7	Al 20	30	4
10	Oishi <i>et al</i> (2005)	0.12	55	6×10^{18}	1×10^5	Cu 5	45	1.3
11	Fuchs <i>et al</i> (2006)	10	320	6×10^{19}	1×10^7	Al 20	0 and 40	20
12	Neely <i>et al</i> (2006)	0.3	33	1×10^{19}	1×10^{10}	Al 0.1	30	4
13	Willingale <i>et al</i> (2006)	340	1000	6×10^{20}	1×10^5	He jet 2000		10
14	Ceccotti <i>et al</i> (2007)	0.65	65	5×10^{18}	1×10^{10}	Mylar 0.1	45	5.25
15	Robson <i>et al</i> (2007)	310	1000	6×10^{20}	1×10^7	Al 10	45	55
16	Robson <i>et al</i> (2007)	160	1000	3.2×10^{20}	1×10^7	Al 10	45	38
17	Robson <i>et al</i> (2007)	30	1000	6×10^{19}	1×10^7	Al 10	45	16
18	Antici <i>et al</i> (2007)	1	320	1×10^{18}	1×10^{11}	Si ₃ N ₄ 0.03	0	7.3
19	Yogo <i>et al</i> (2007)	0.71	55	8×10^{18}	1×10^6	Cu 5	45	1.4
20	Yogo <i>et al</i> (2008)	0.8	45	1.5×10^{19}	2.5×10^5	Polyimide 7.5	45	3.8
21	Nishiuchi <i>et al</i> (2008)	1.7	34	3×10^{19}	2.5×10^7	Polyimide 7.5	45	4
22	Flippo <i>et al</i> (2008)	20	600	1.1×10^{19}	1×10^6	Flat-top cone Al 10	0	30
23	Safronov <i>et al</i> (2008)	6.5	900	1×10^{19}		Al 2	0	8
24	Henig <i>et al</i> (2009b)	0.7	45	5×10^{19}	1×10^{11}	DLC 0.0054	0	13
25	Fukuda <i>et al</i> (2009)	0.15	40	7×10^{17}	1×10^6	CO ₂ +He cluster jet 2000		10
26	Zeil <i>et al</i> (2010)	3	30	1×10^{21}	2×10^8	Ti 2 μm	45	17
27	Gaillard <i>et al</i> (2011)	82	670	1.5×10^{20}	1×10^9	Flat-top cone Cu 12.5	0	67.5

¹⁰

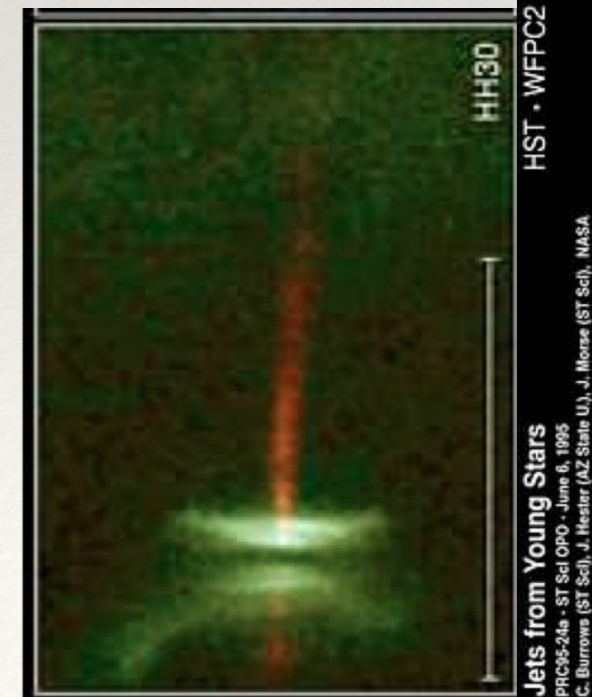
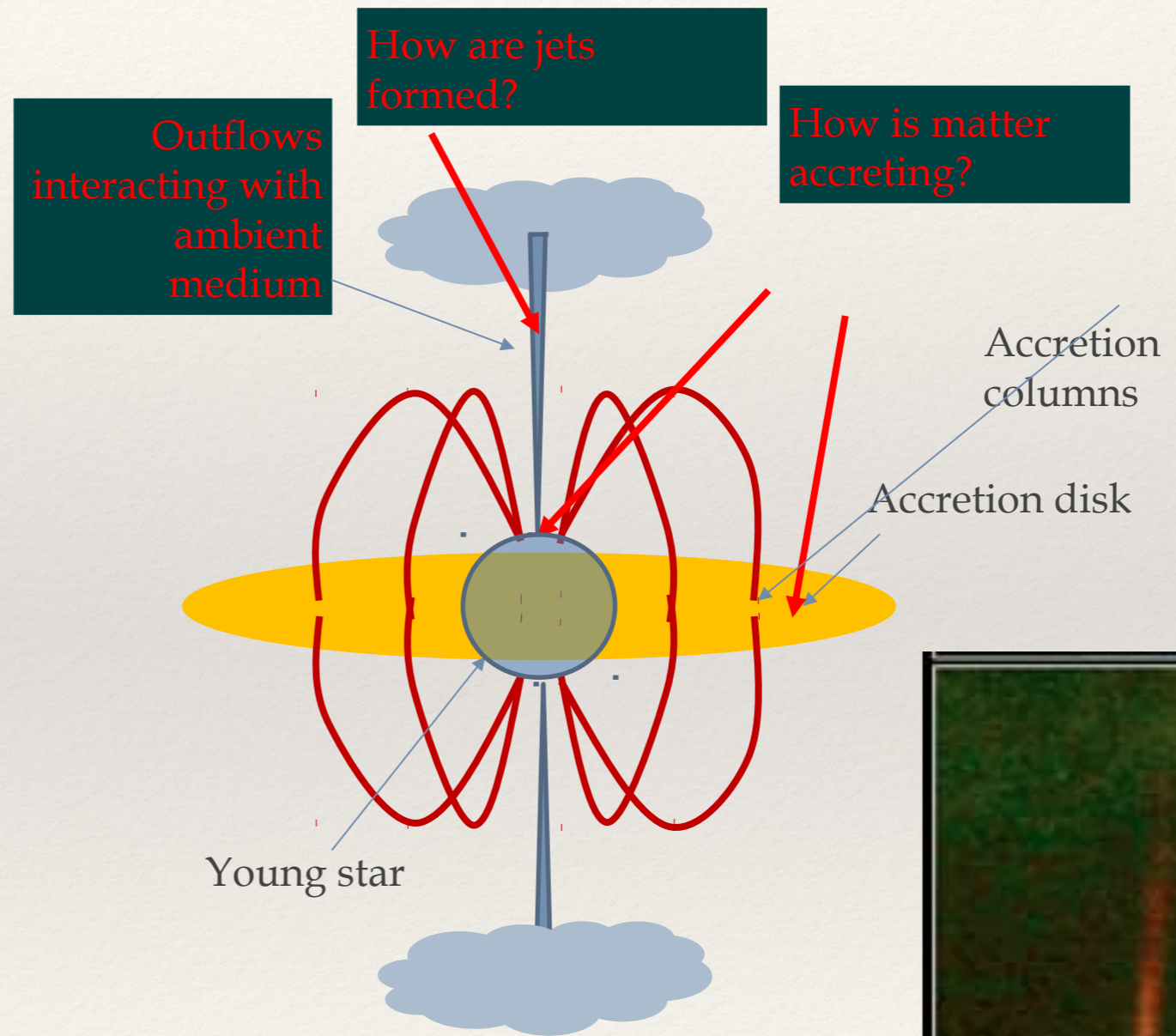
Laser-plasma interaction: applications

- ❖ Laser driven acceleration
- ❖ Particles acceleration
- ❖ X-ray generation.
- ❖ Applications
 - ❖ Radiotherapy
 - ❖ Bio-imaging
- ❖ HED physics
 - ❖ LabAstro
 - ❖ ICF



Laboratory astrophysics

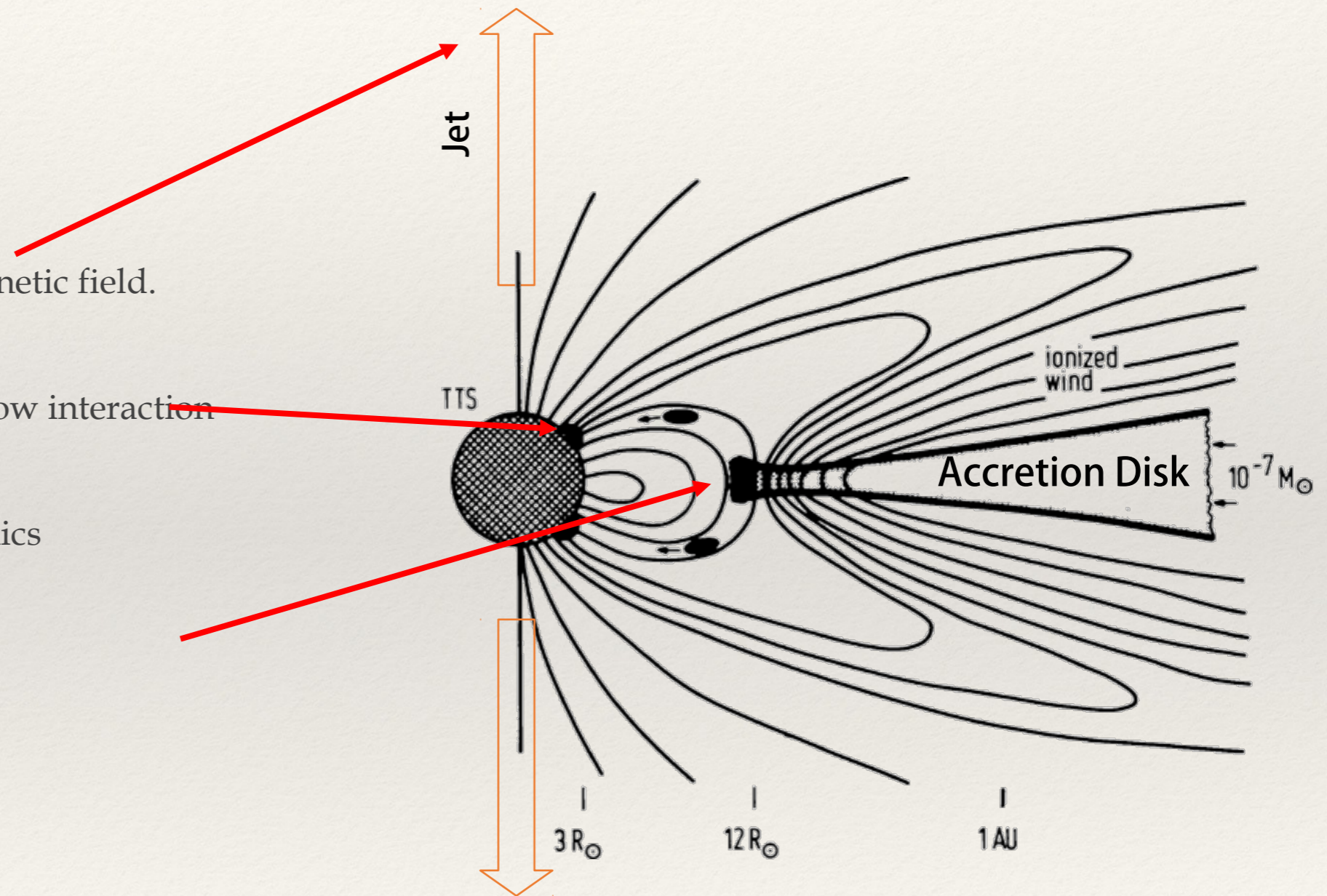
- ❖ Modeling of magneto-hydrodynamic plasma phenomena



Laboratory astrophysics

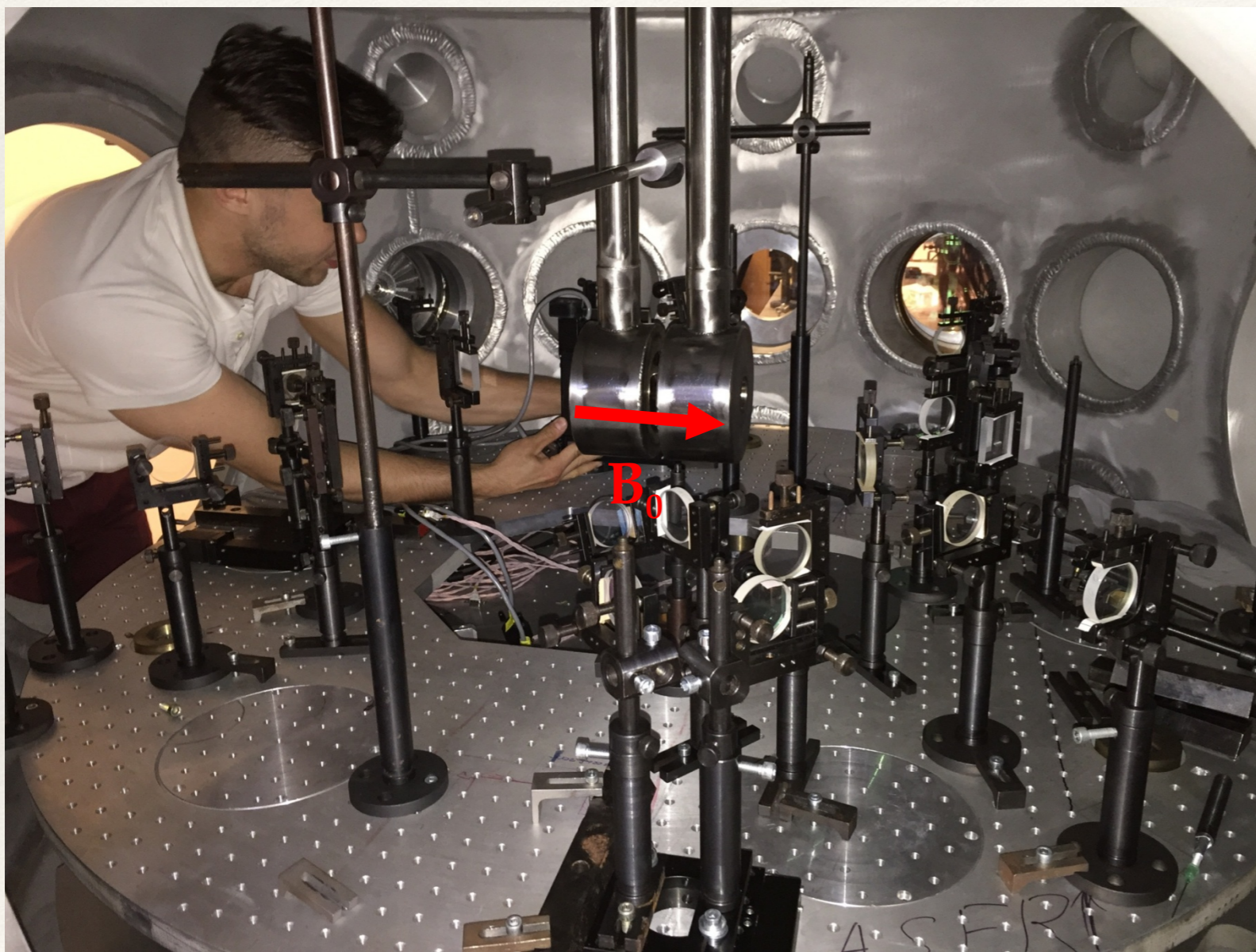
❖ Modeling of magneto-hydrodynamic plasma phenomena

- Jet formation:
effect of poloidal magnetic field.
- Accretion column:
magnetized plasma flow interaction
with surface.
- Accretion disc dynamics
in the vicinity of $\beta \sim 1$.



Laboratory astrophysics

- ❖ Modeling of magneto-hydrodynamic plasma phenomena



Ambient magnetic field

- Split pulsed solenoid
- Uniform configuration (20 T)
- “Zero-point” configuration

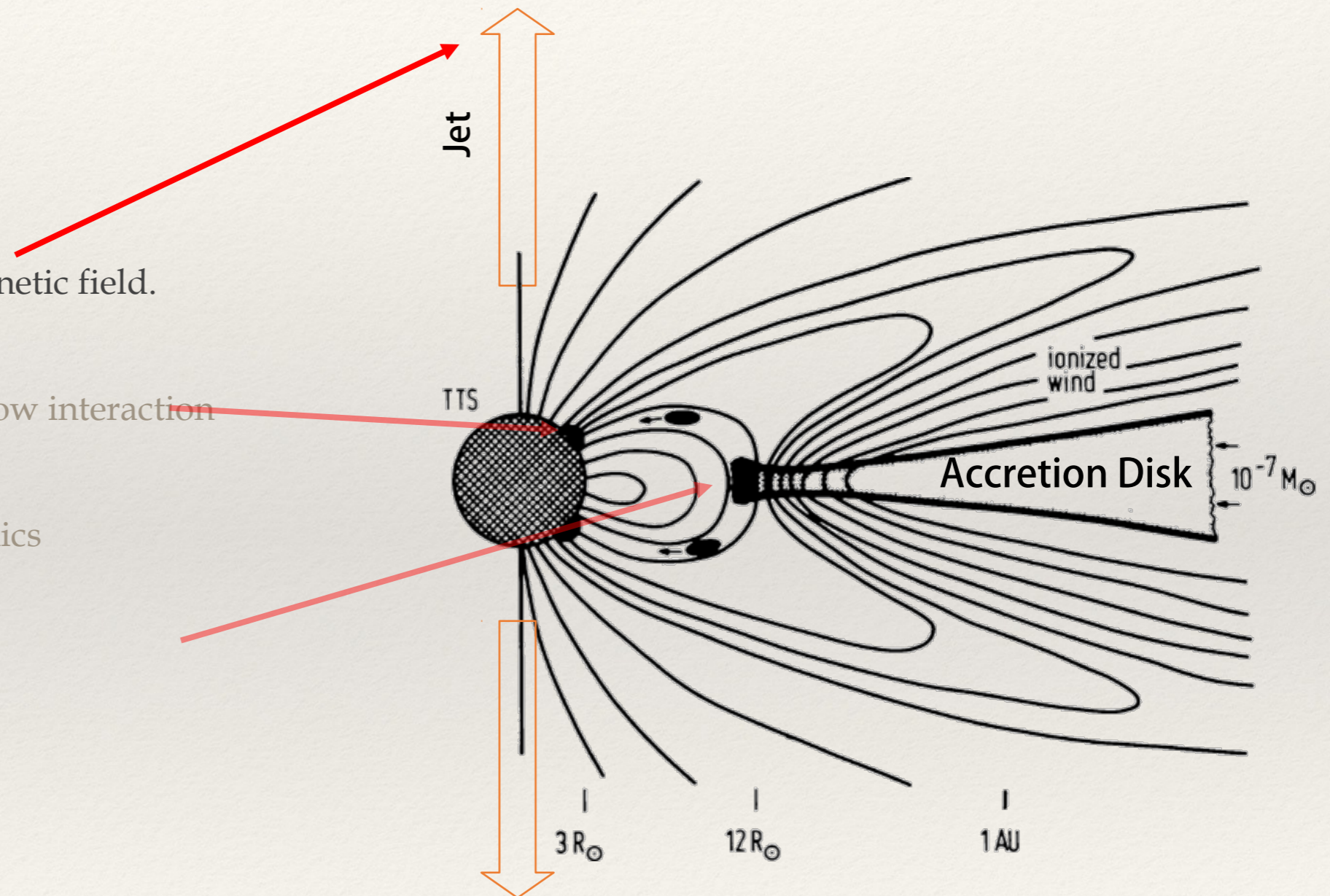
Laser plasma production

- PEARL pump laser (~100 J, 1 ns, 1054 nm)
- Solid-state targets

Laboratory astrophysics

❖ Modeling of magneto-hydrodynamic plasma phenomena

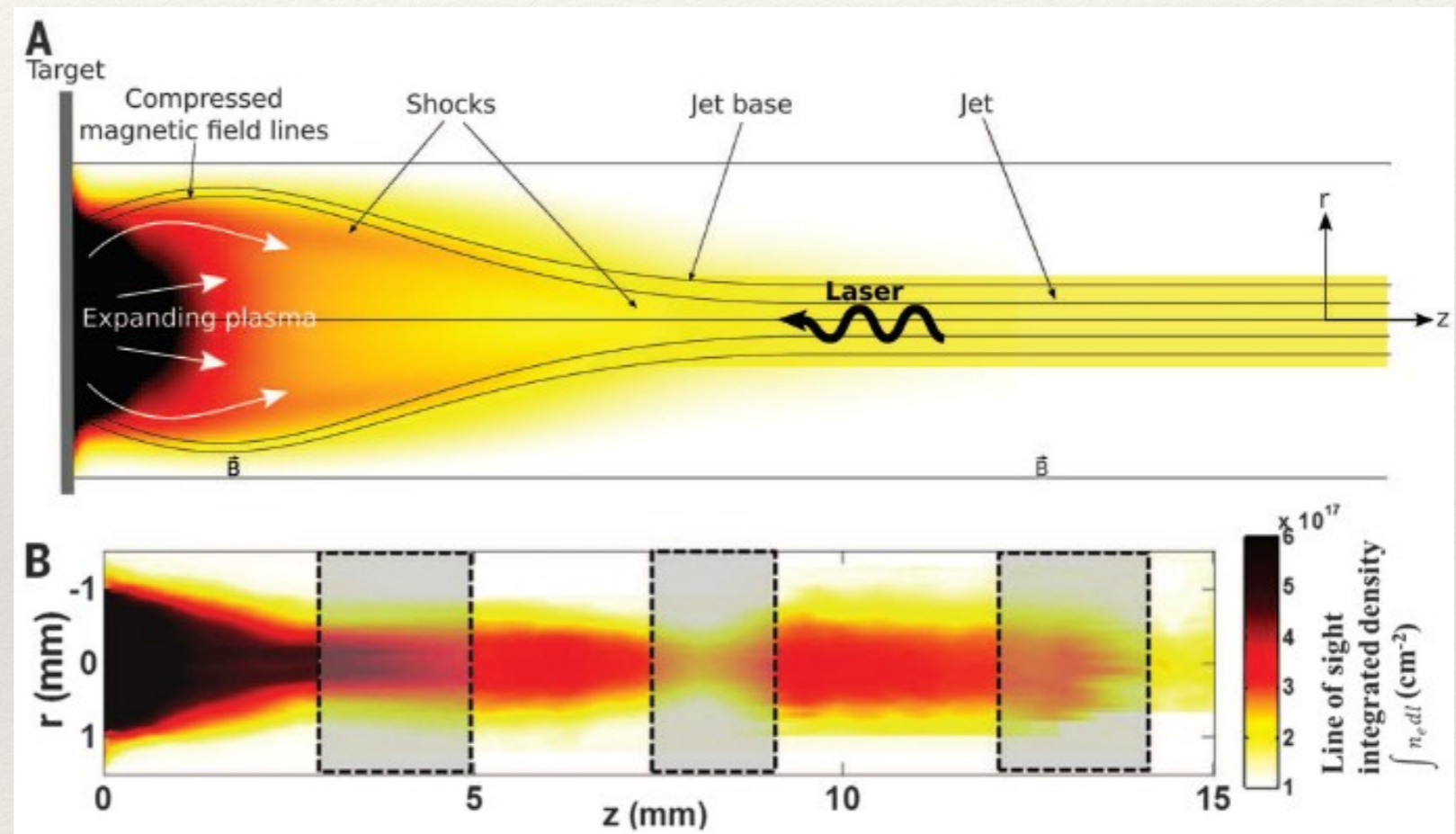
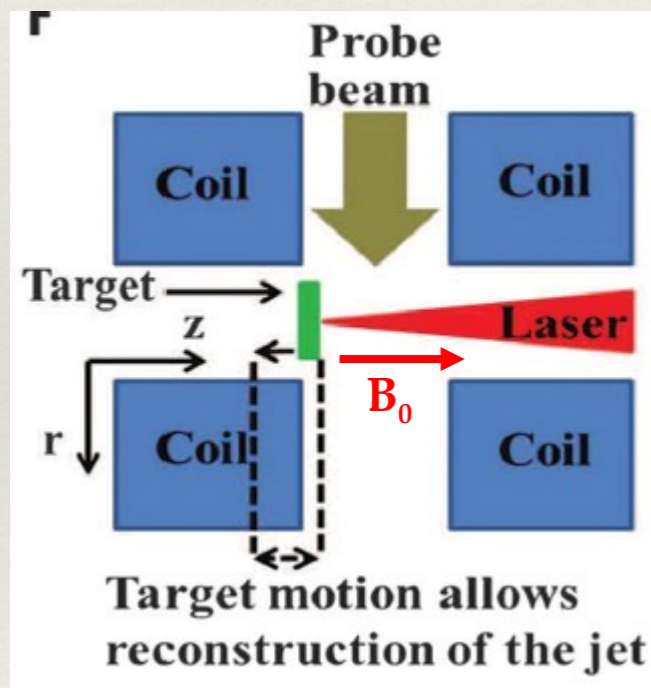
- Jet formation: effect of poloidal magnetic field.
- Accretion column: magnetized plasma flow interaction with surface.
- Accretion disc dynamics in the vicinity of $\beta \sim 1$.



Laboratory astrophysics

- Modeling of magneto-hydrodynamic plasma phenomena: **jet formation mechanisms**

Laser-plasma plume propagating along the ambient magnetic field



Laboratory formation of a scaled protostellar jet by coaligned poloidal magnetic field

B. Albertazzi *et al.*

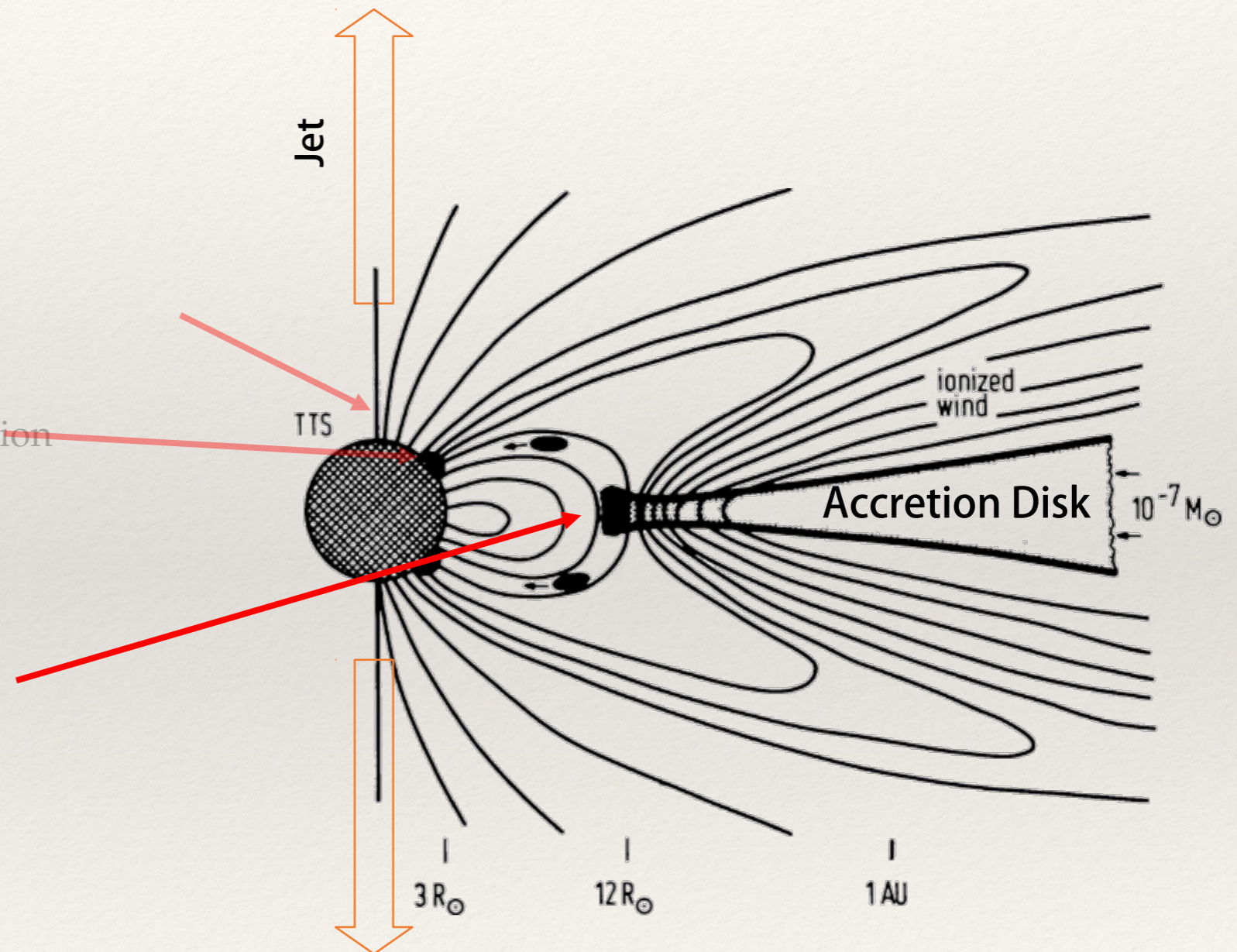
Science **346**, 325 (2014);

DOI: 10.1126/science.1259694

Laboratory astrophysics

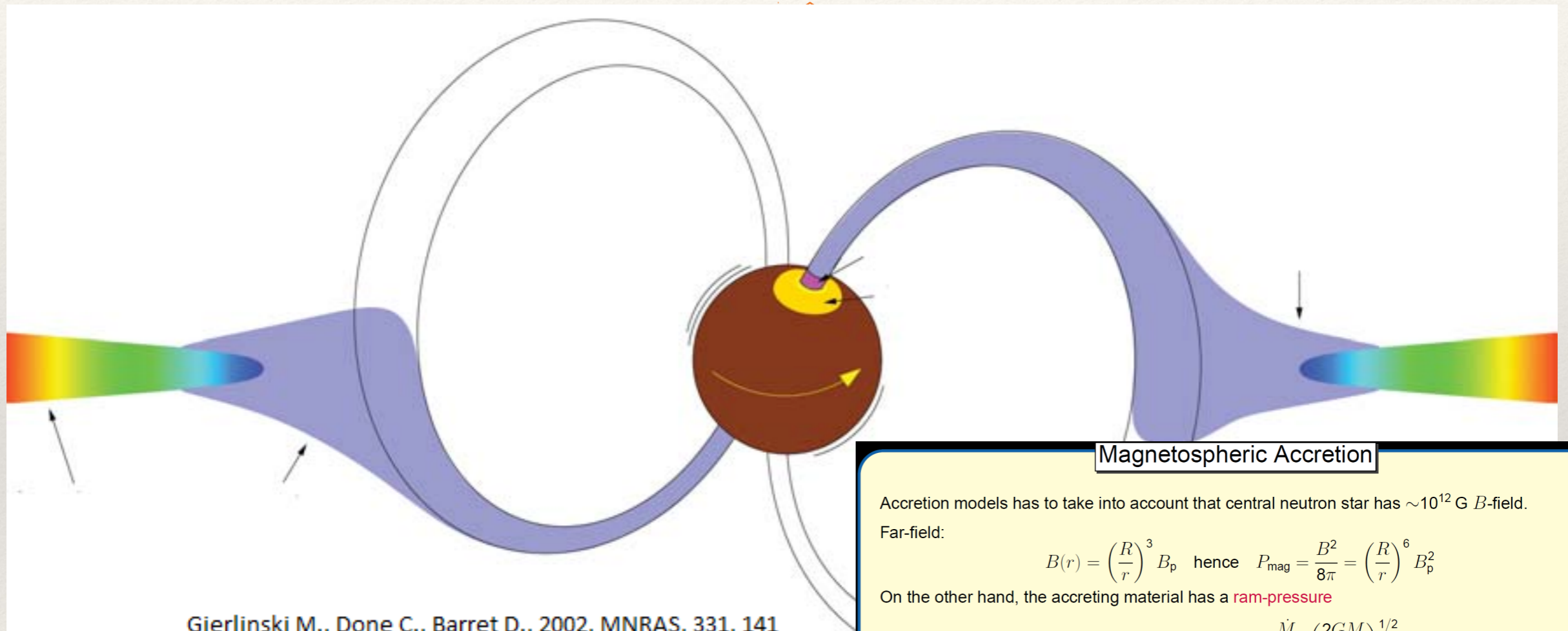
❖ Modeling of magneto-hydrodynamic plasma phenomena

- Jet formation:
effect of poloidal magnetic field.
- Accretion column:
magnetized plasma flow interaction
with surface.
- Accretion disc dynamics
in the vicinity of $\beta \sim 1$.



Laboratory astrophysics

- ❖ Modeling of magneto-hydrodynamic plasma phenomena



Gierlinski M., Done C., Barret D., 2002, MNRAS, 331, 141

Magnetospheric Accretion

Accretion models has to take into account that central neutron star has $\sim 10^{12}$ G B -field.

Far-field:

$$B(r) = \left(\frac{R}{r}\right)^3 B_p \quad \text{hence} \quad P_{\text{mag}} = \frac{B^2}{8\pi} = \left(\frac{R}{r}\right)^6 B_p^2$$

On the other hand, the accreting material has a **ram-pressure**

$$P_{\text{ram}} = \rho v^2 \quad \text{or} \quad P_{\text{ram}} = \frac{\dot{M}}{4\pi r^2} \left(\frac{2GM}{r}\right)^{1/2}$$

assuming **free fall** ($v = (2GM/r)^{1/2}$) and **spherical symmetry** ($\dot{M} = 4\pi r^2 \rho v$).

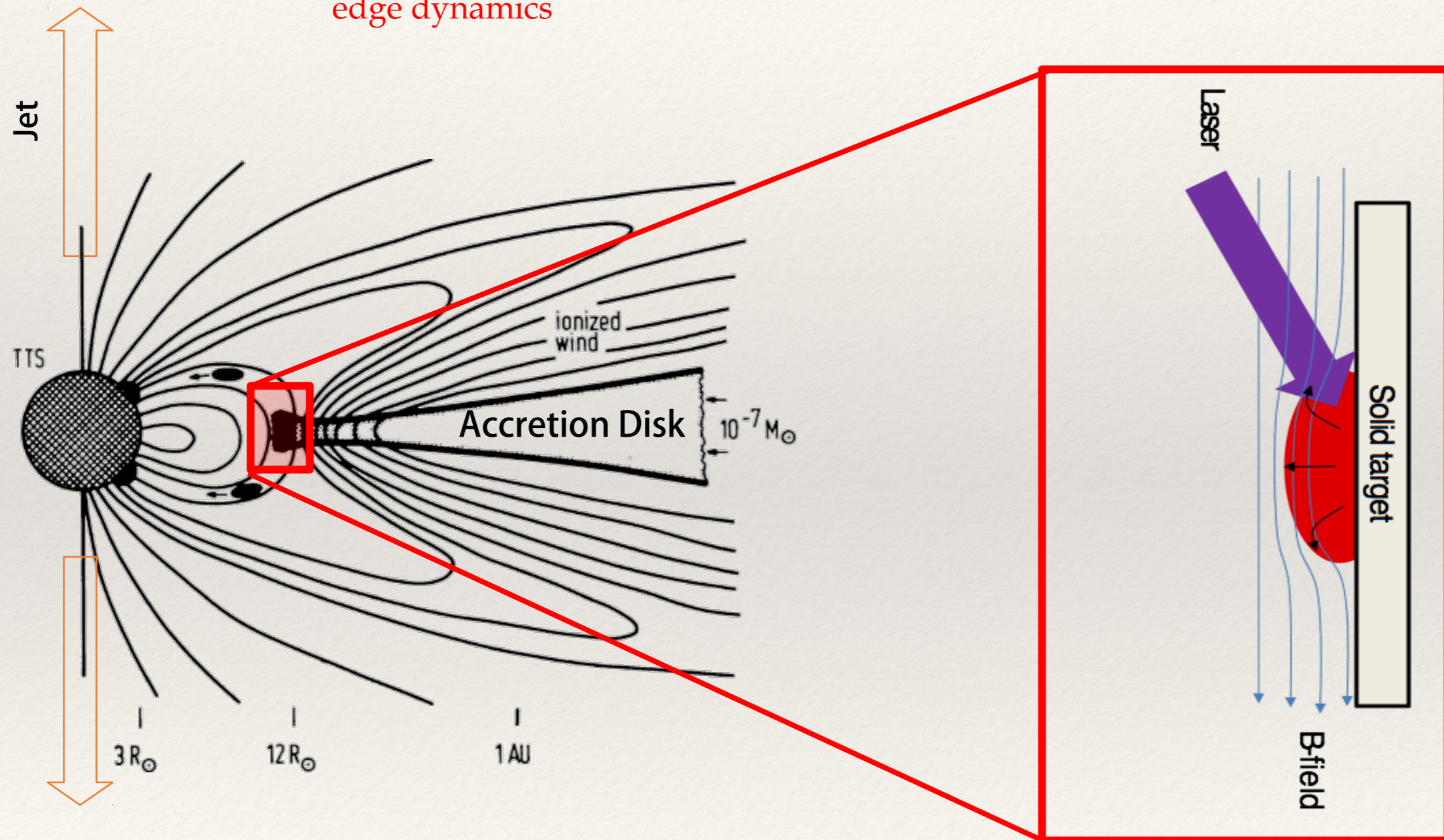
For $P_{\text{mag}} > P_{\text{ram}}$, **B -field dominates** \implies **plasma couples to B -field lines** at the **Alfvén radius**

$$\begin{aligned} r_{\text{mag}} &= \left(\frac{8\pi^2}{G}\right)^{1/7} \left(\frac{R^{12} B_p^4}{M \dot{M}^2}\right)^{1/7} \\ &= 1800 \text{ km} \left(\frac{R}{10 \text{ km}}\right)^{12/7} \left(\frac{B}{10^{12} \text{ G}}\right)^{4/7} \left(\frac{M}{1.4 M_\odot}\right)^{-1/7} \left(\frac{\dot{M}}{10^{-7} M_\odot \text{ yr}^{-1}}\right)^{-2/7} \end{aligned}$$

For typical NS parameters, the accretion close to the NS is dominated by the B -field.

Laboratory astrophysics

- Modeling of magneto-hydrodynamic plasma phenomena: **accretion disc edge dynamics**

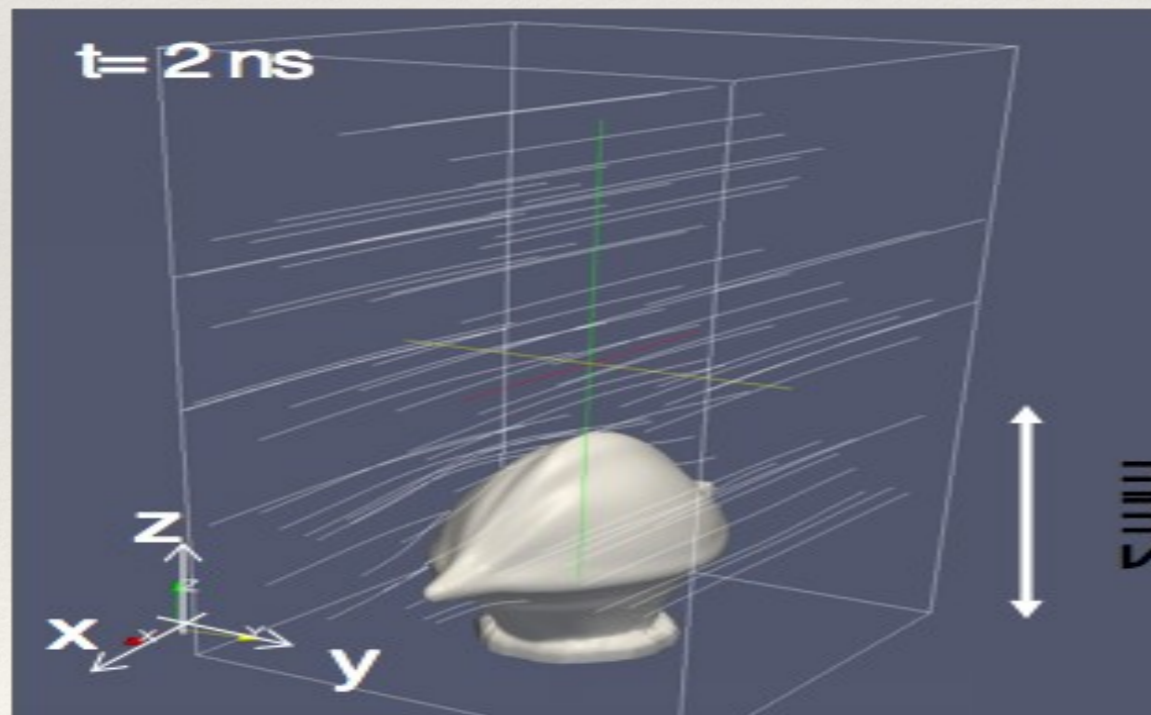
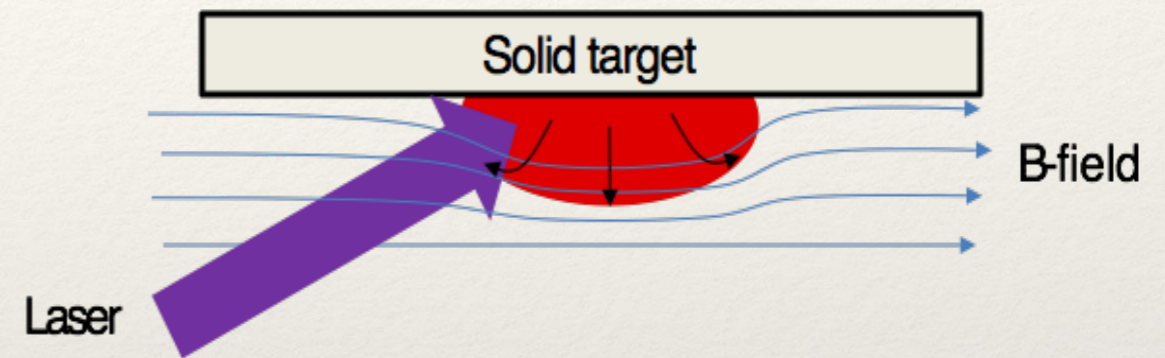


Adapted from Camenzind, (1990).

Laboratory astrophysics

- Modeling of magneto-hydrodynamic plasma phenomena: **accretion disc**
edge dynamics

Laser-plasma plume
propagating across
the ambient magnetic field



expect:

plasma expansion across \mathbf{B}_0
is limited by magnetic pressure

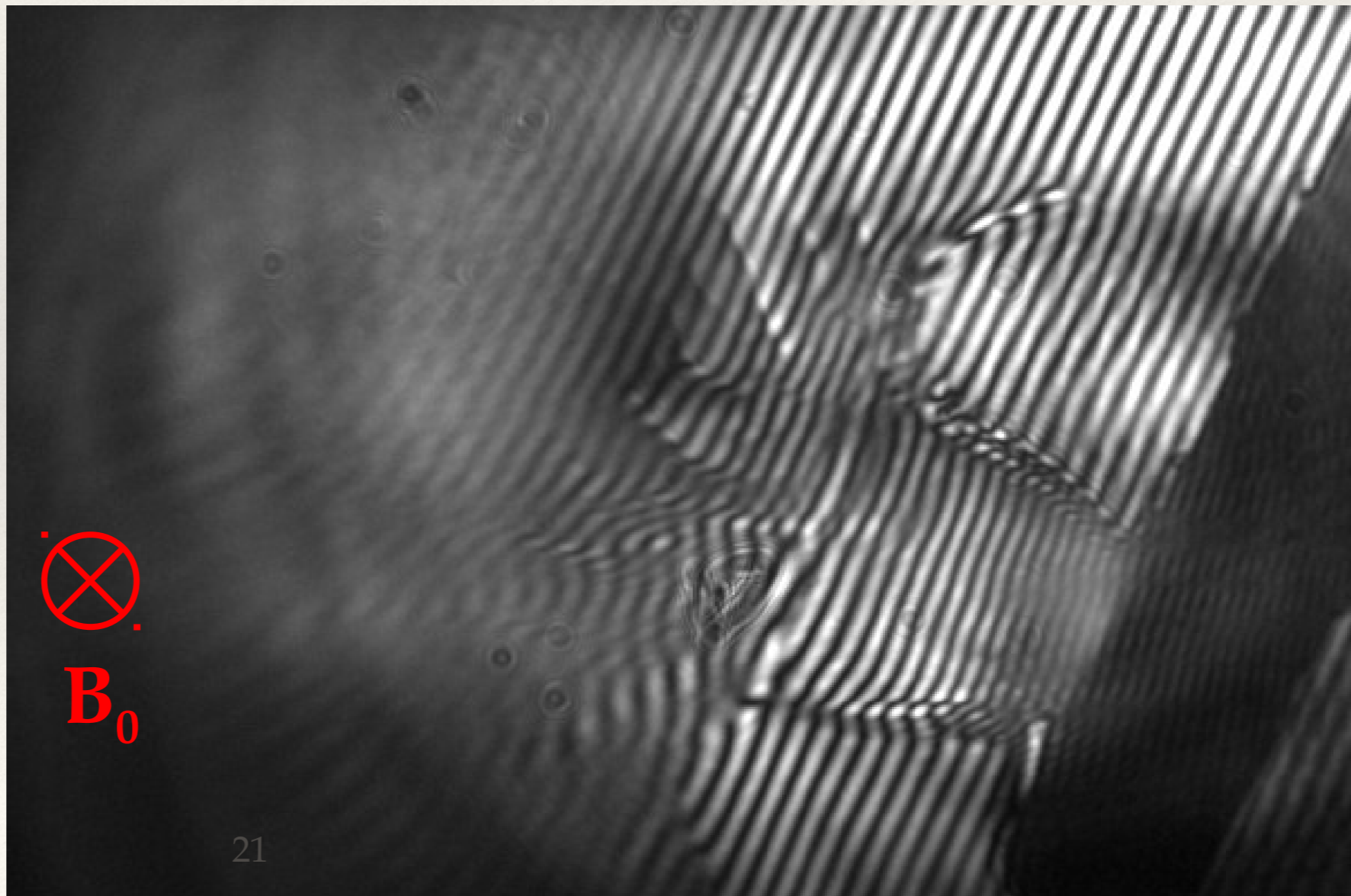
further plasma expansion
is along \mathbf{B}_0

Andrea Ciardi (2016)

Laboratory astrophysics

- ❖ Modeling of magneto-hydrodynamic plasma phenomena: accretion disc

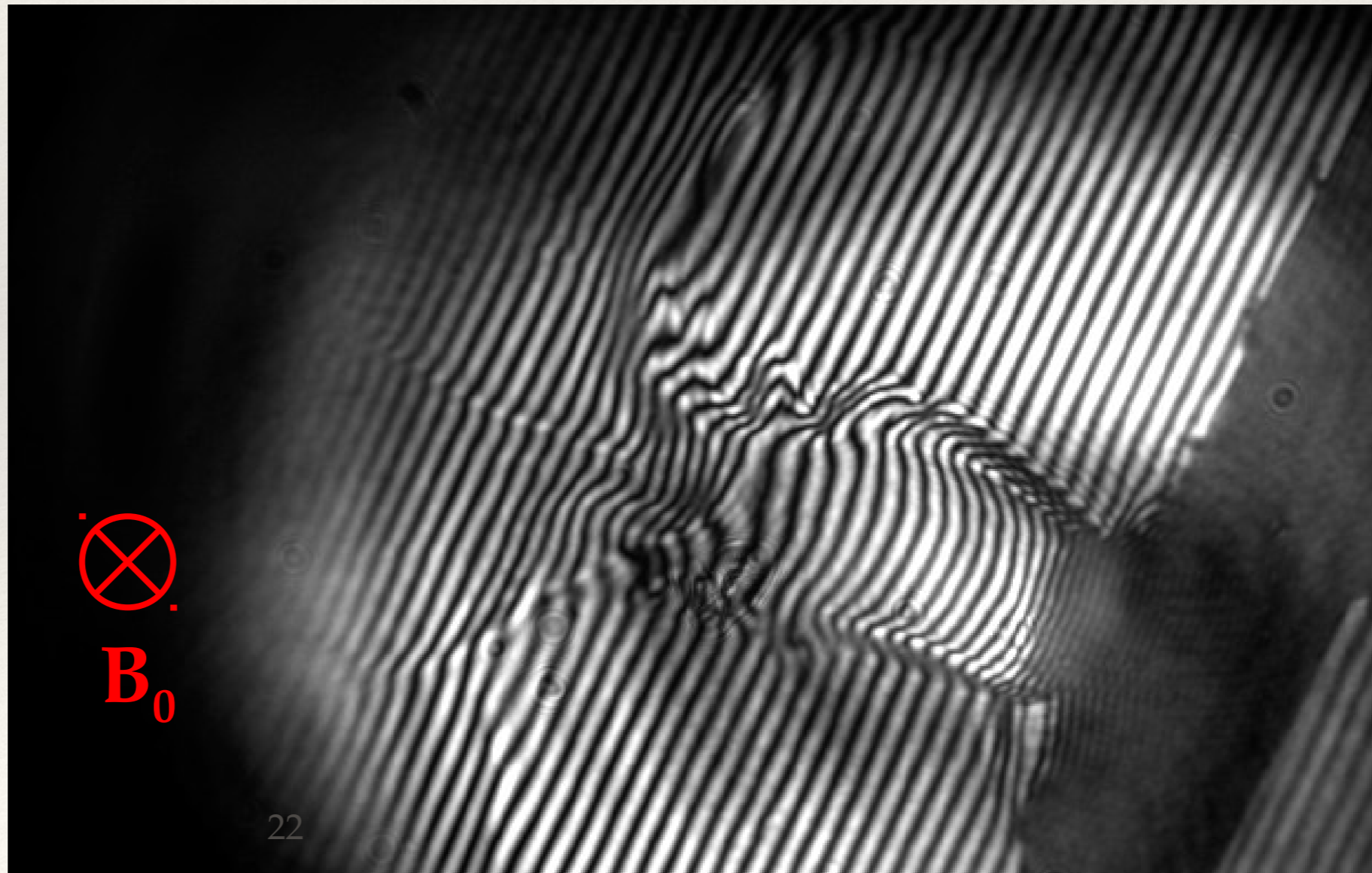
16ns,
25J



Laboratory astrophysics

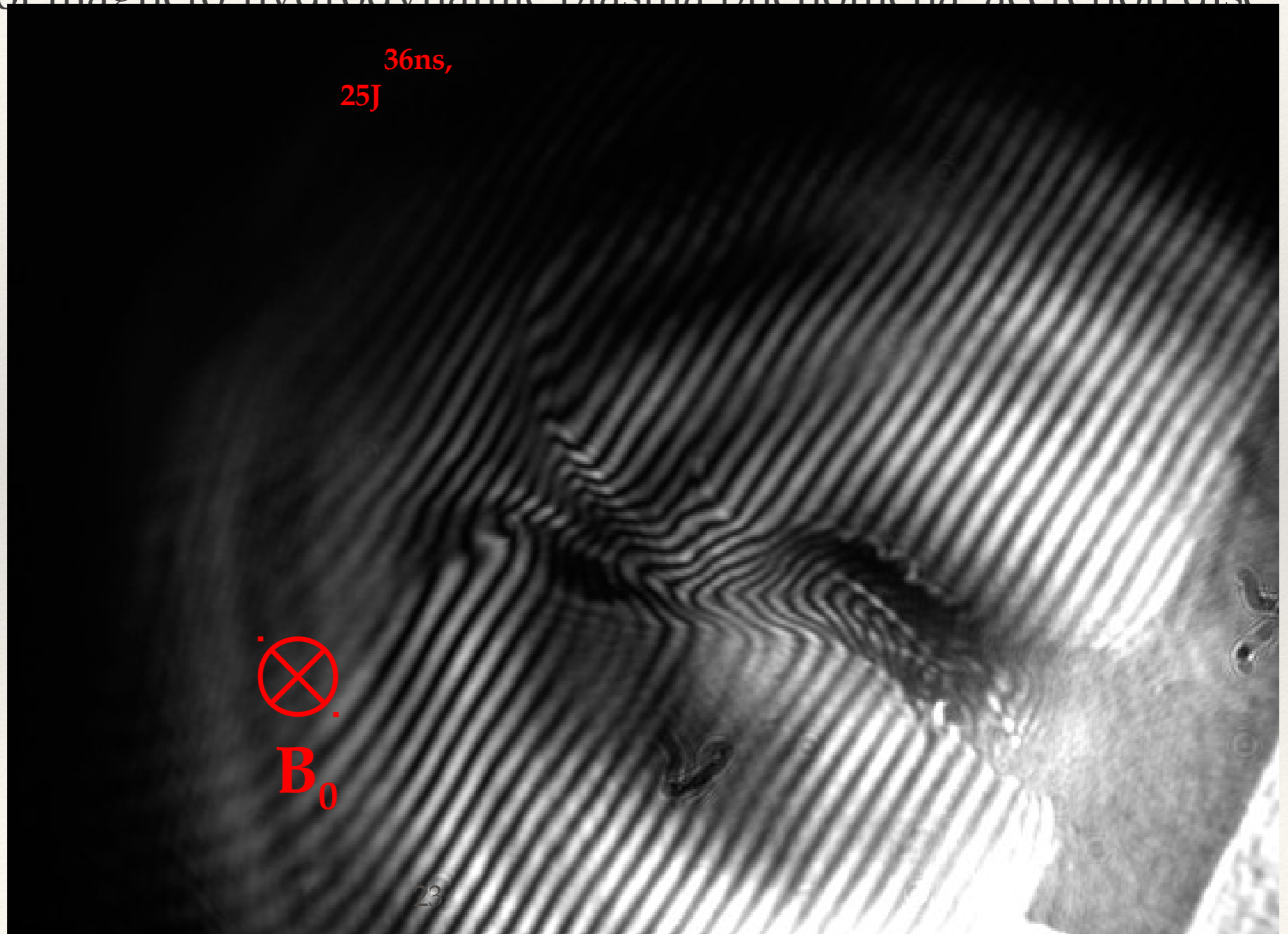
- ❖ Modeling of magneto-hydrodynamic plasma phenomena: accretion disc

26ns,
25J



Laboratory astrophysics

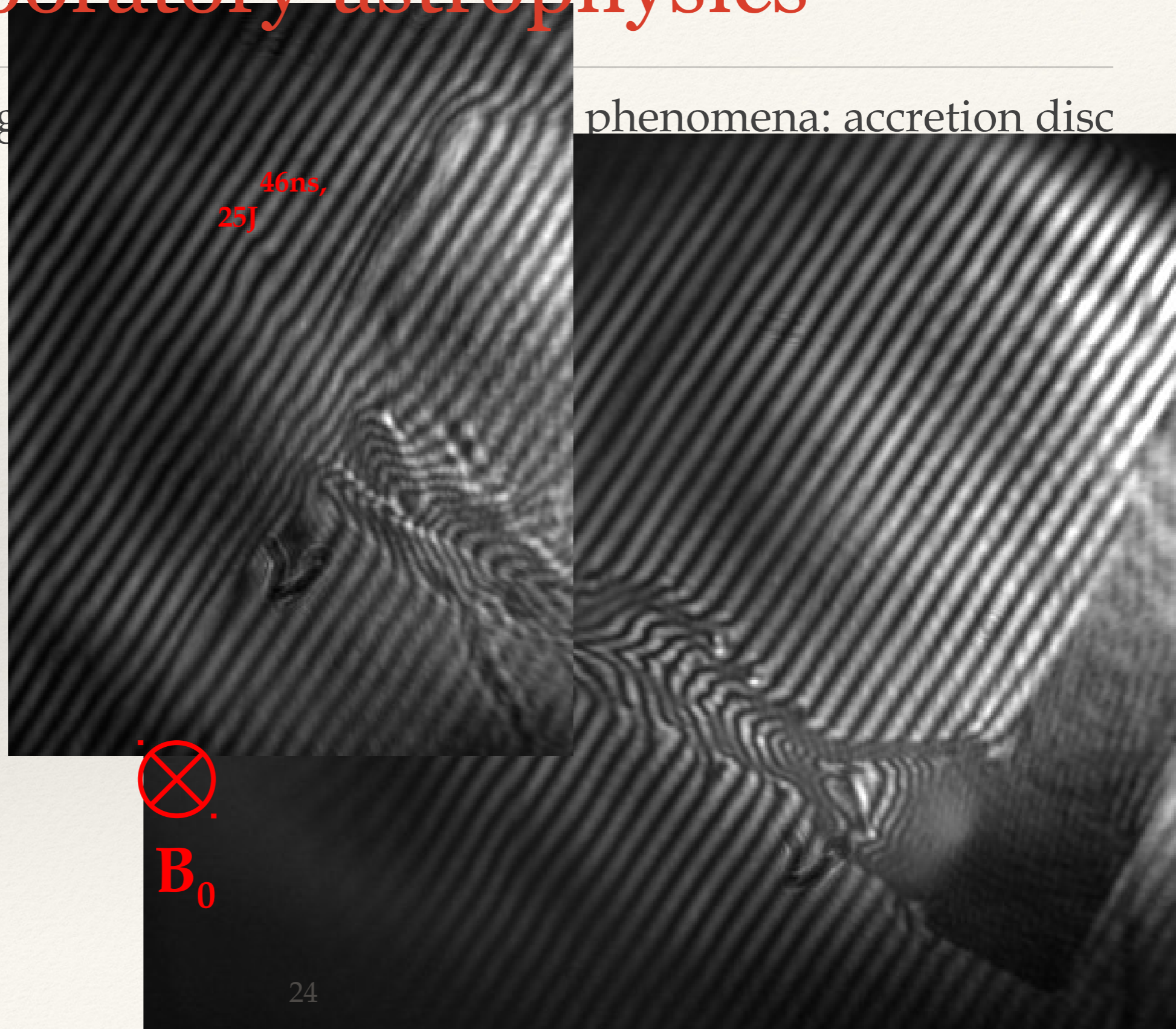
- ❖ Modeling of magneto-hydrodynamic plasma phenomena: accretion disc



Laboratory astrophysics

- ❖ Modeling of mag

phenomena: accretion disc



Laboratory astrophysics

tion disc

56ns,
25J


 B_0

Laboratory astrophysics

phenomena: accretion disc

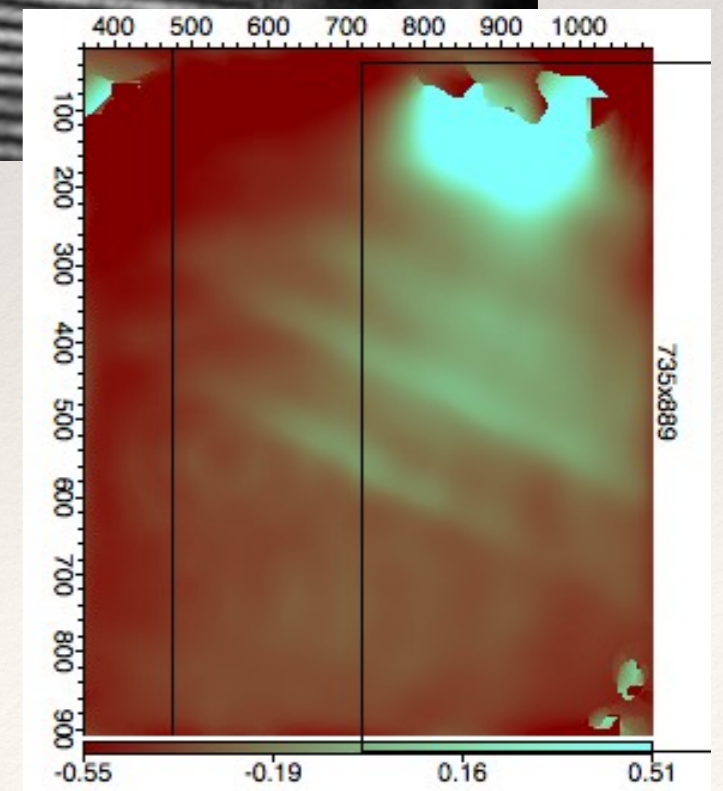
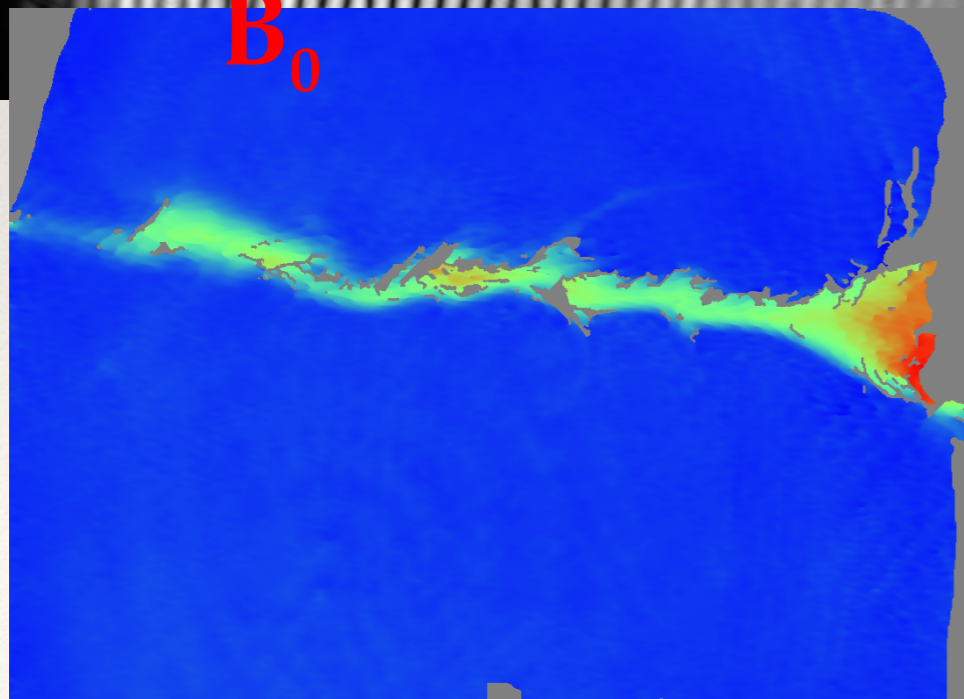
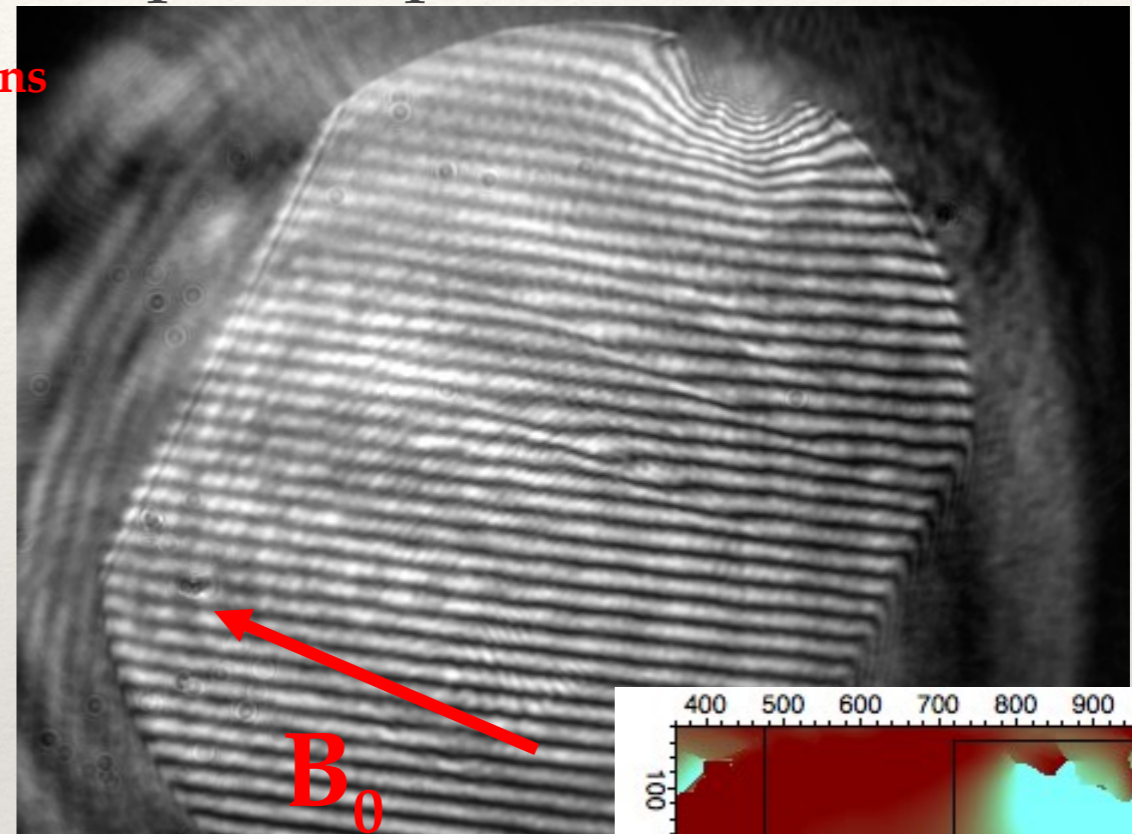
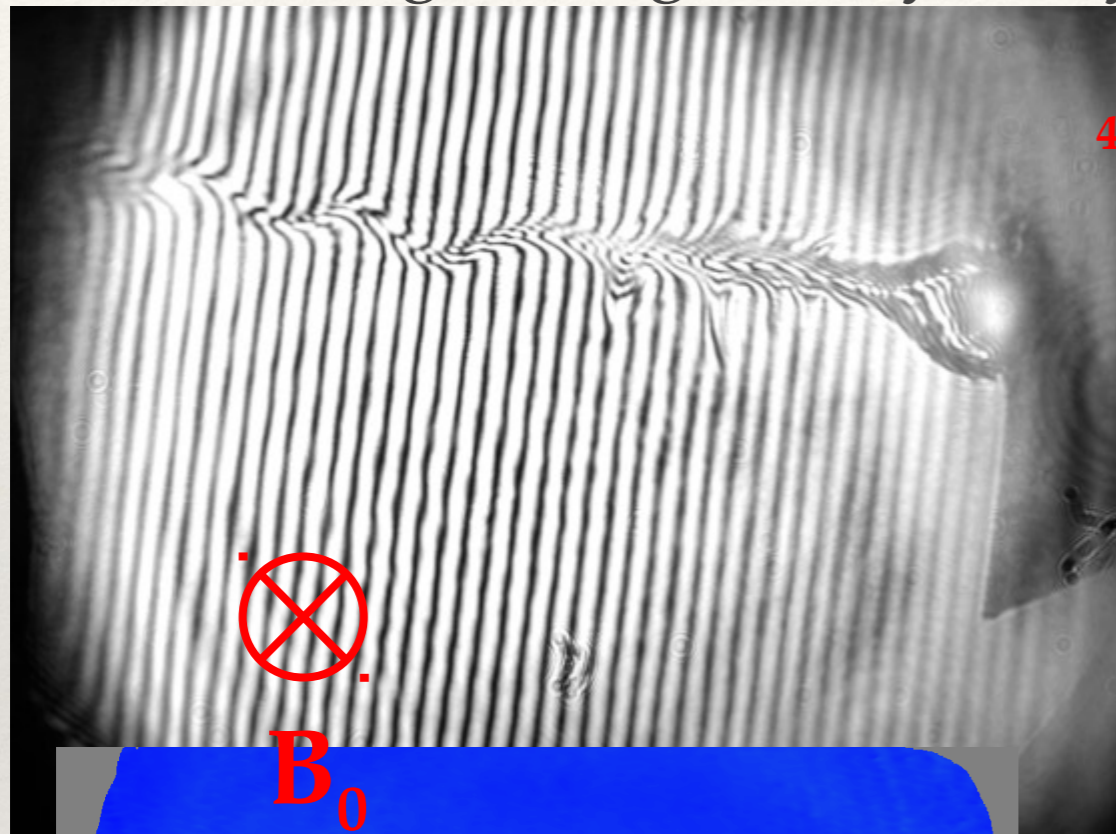
76ns,
25J



B_0

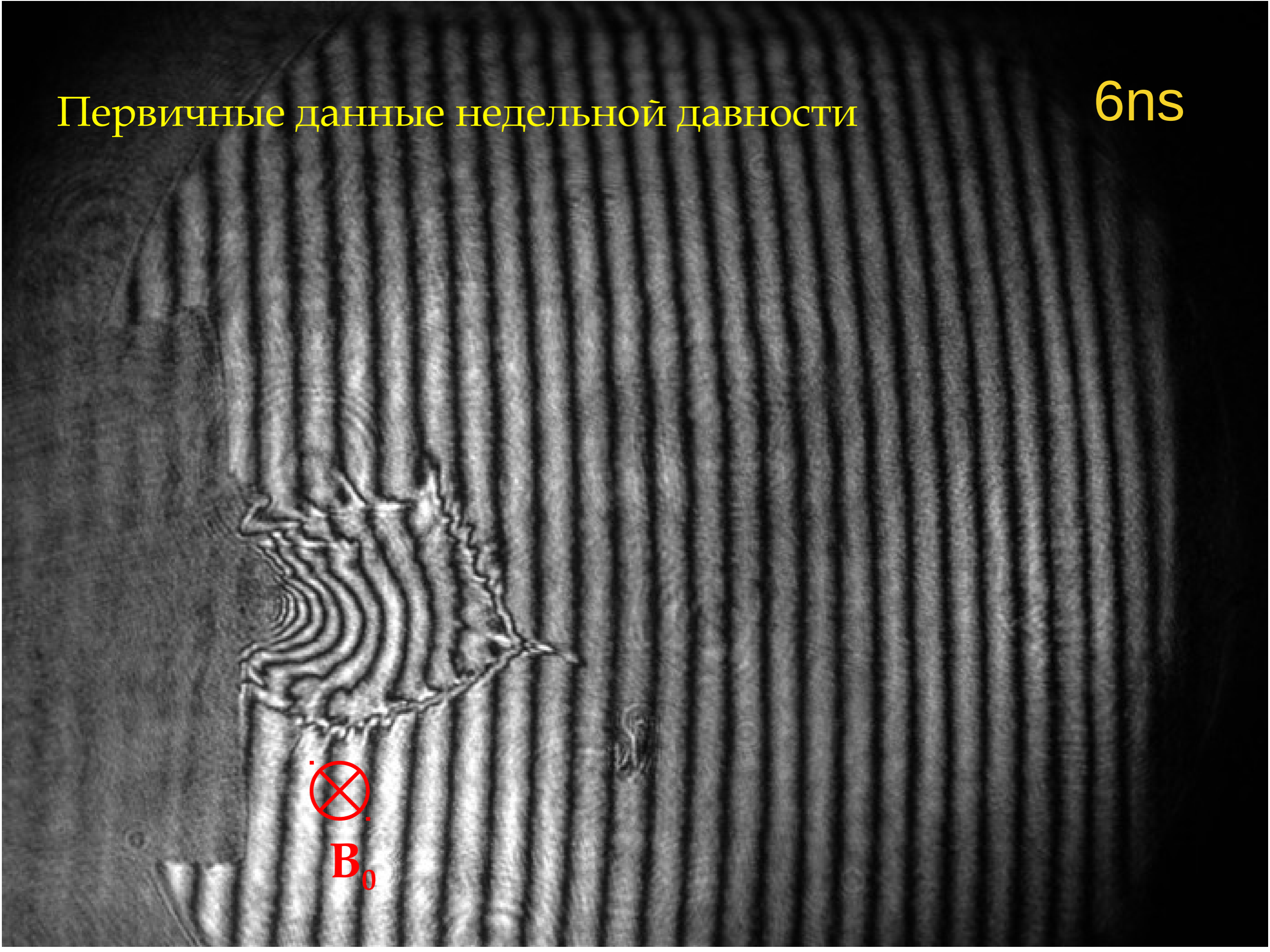
Laboratory astrophysics

- ❖ Modeling of magneto-hydrodynamic plasma phenomena: accretion disc



Первичные данные недельной давности

6ns



Первичные данные недельной давности

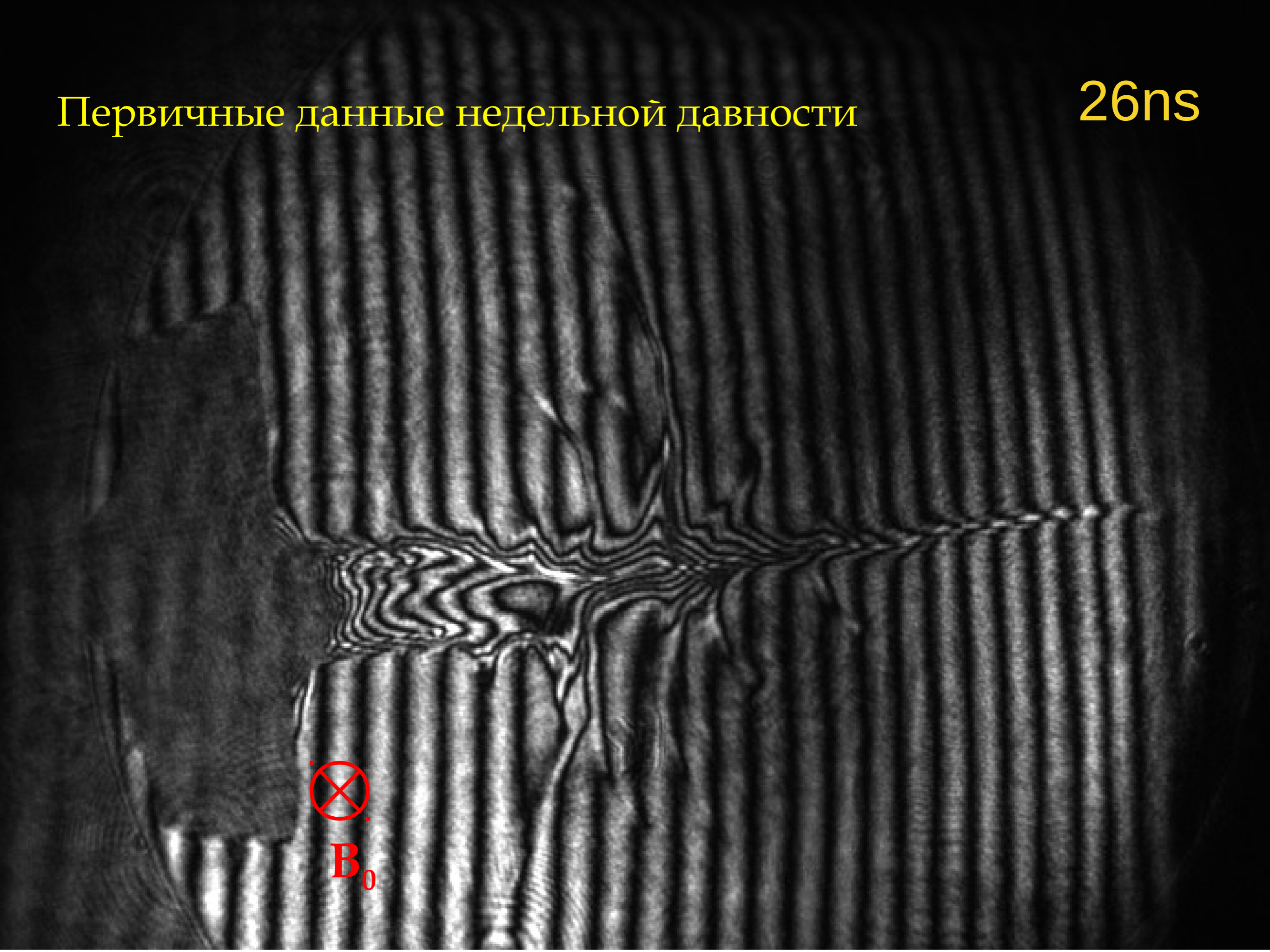
16ns



B_0

Первичные данные недельной давности

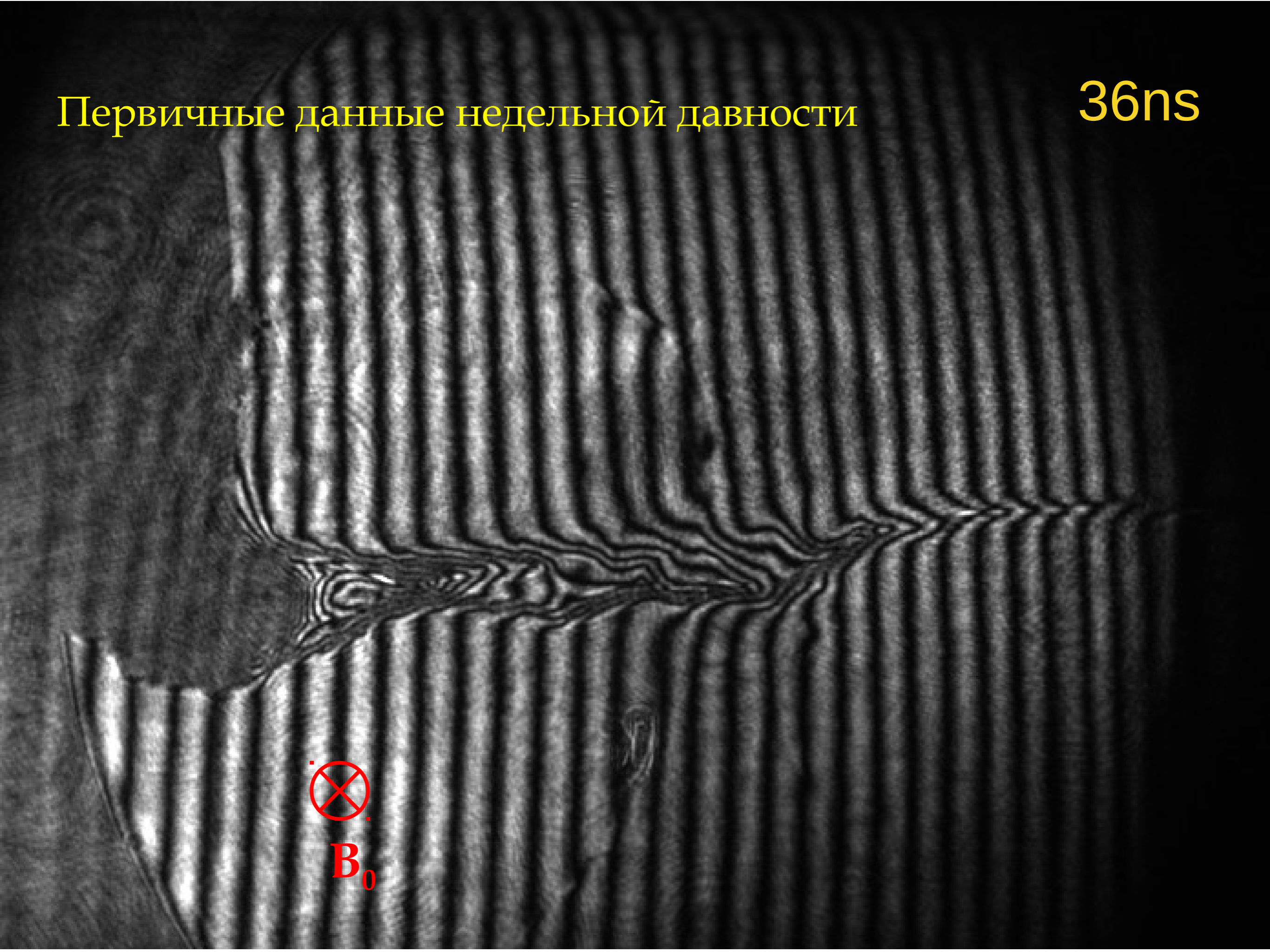
26ns



B_0

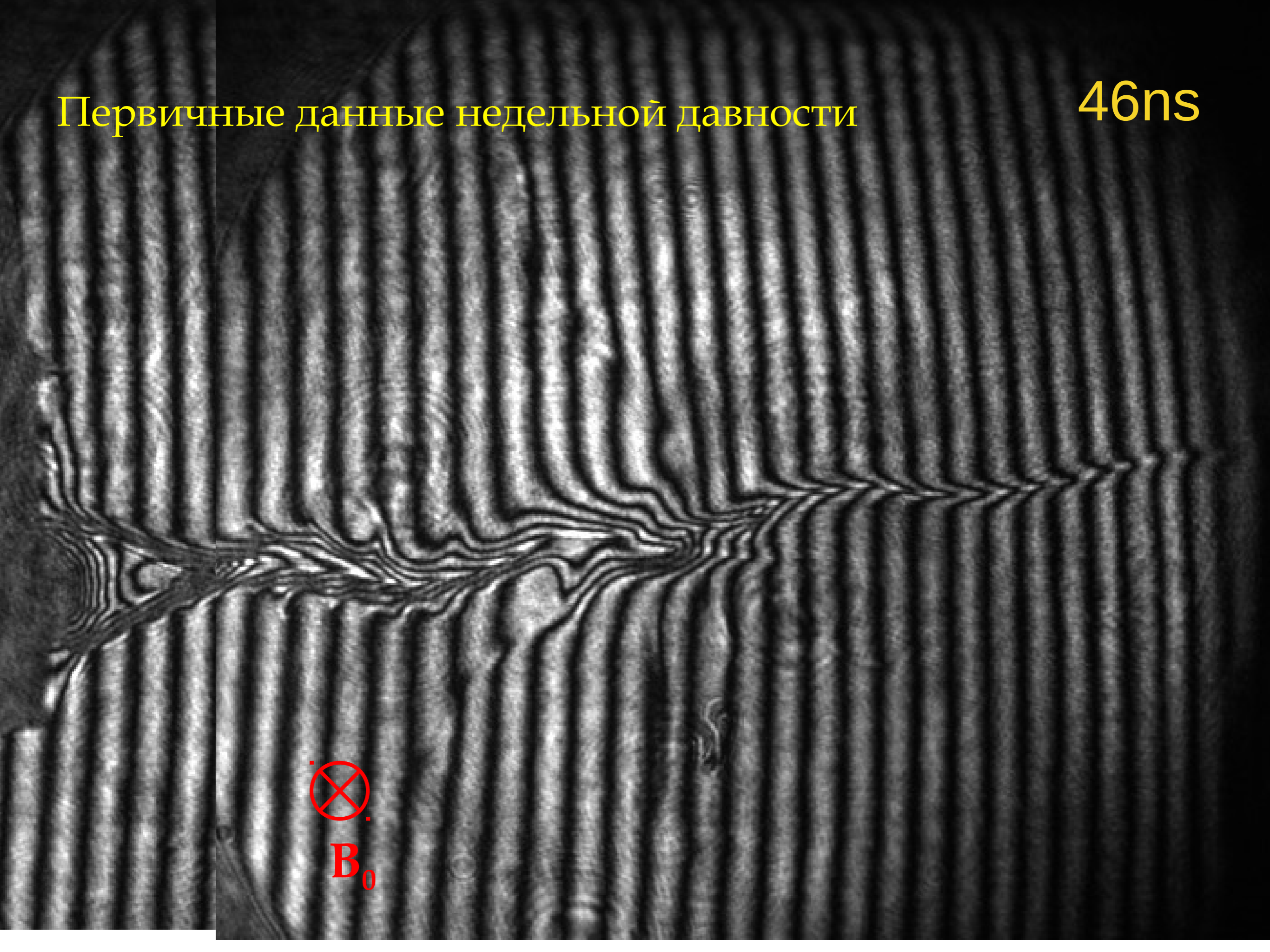
Первичные данные недельной давности

36ns



Первичные данные недельной давности

46ns



B_0

Laboratory astrophysics

- ❖ Modeling of magneto-hydrodynamic plasma phenomena

Main dynamics:
RT instability ?

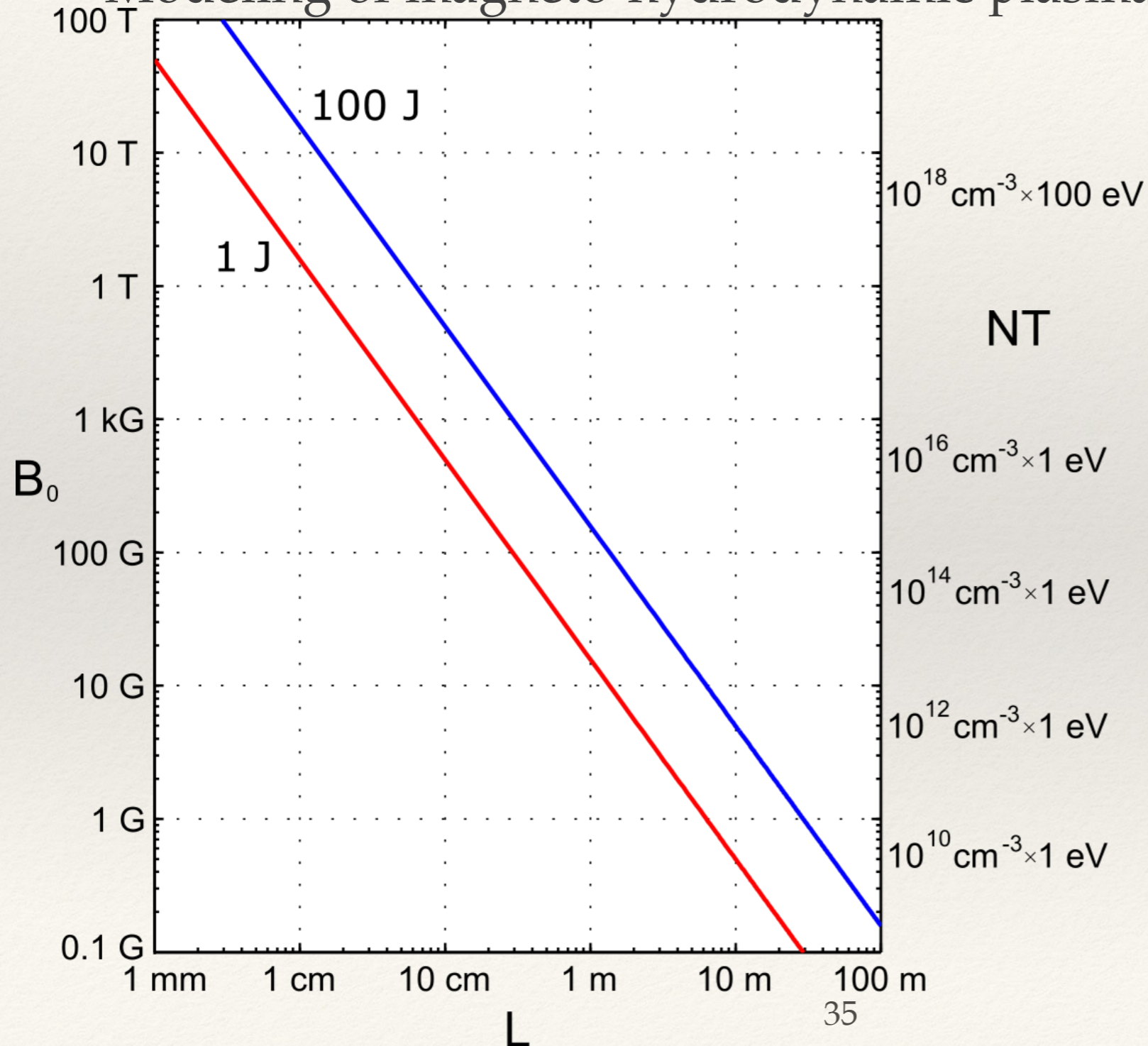
Side oscillations:
KH instability ?

**Where are the accretion columns ?
Are the astrophysical accretion
models correct ?**

<i>Incident stream</i>	Laboratory	CTTS
	B-Field = 20T	B-Field = $1 \times 10^{-3}T$
Material	C_2H_3Cl	H
Electronic density [$n. cm^{-3}$]	1.5×10^{18}	1×10^{11}
Temperature [eV]	10	2.6×10^{-1}
Density [$g. cm^{-3}$]	8×10^{-6}	1.7×10^{-13}
Speed accertion flow [$km. s^{-1}$]	1000	500
Sound speed [$km. s^{-1}$]	21	13
Mach number	45	38
Reynolds	2×10^6	1×10^9
Peclet number	6×10^3	5×10^7
Magnetic Reynolds	2×10^2	1×10^9
β	1.5×10^{-2}	6×10^{-2}
l_c/L	7×10^{-3}	2×10^{-8}
Euler number ($v\sqrt{\rho/p}$)	6×10^1	5×10^1
Alfven number ($B/\sqrt{\rho}$)	2×10^2	1×10^2

Laboratory astrophysics

❖ Modeling of magneto-hydrodynamic plasma phenomena: scaling



$$W = NTL^3$$

NT

$$NT = B^2 / 8\pi$$

Основные результаты

- ❖ Российский лазерный комплекс PEARL активно используется для широкого спектра исследований в области лазерной физики, физики плазмы, в частности среды с высокой плотностью энергии. В частности:
- ❖ Проведены экспериментальные исследования лазерного ускорения частиц (электронов и протонов), которые станут основой большого числа прикладных исследований в области медицины, HED физики и пр.
- ❖ В настоящее время продолжаются экспериментальные исследования распространения плазмы поперек магнитного поля, способные пролить свет на фундаментальные вопросы динамики образования звезд и ряда других актуальных задач.